

Research article



Survival strategies of shrubby seablite (*Suaeda vera*) for ecological success in hypersaline habitats

Naila Asghar^a, Zhen Liu^a, Amina Ameer^b, Khawaja Shafique Ahmad^c, Ummar Iqbal^d, Mansoor Hameed^d, Ying Shen^a, Zhao Hongxiang^a, Muhammad Kaleem^e, Tangyuan Ning^{a,*}

^a College of Agronomy, Shandong Agricultural University, Taian, 271018, Shandong Province, China

^b College of Geography and Environmental Science, Henan University, Kaifeng, 475004, China

^c Department of Botany, University of Poonch Rawalakot, Rawalakot, 12350, AJK, Pakistan

^d Department of Botany, The Islamia University of Bahawalpur, Rahim Yar Khan Campus, Bahawalpur, 64200, Pakistan

^e Department of Botany, University of Agriculture, Faisalabad, 38040, Pakistan

ARTICLE INFO

Keywords:

Salt accumulator
Succulent halophyte
Saline habitats
Adaptative strategies
Mesophyll tissues

ABSTRACT

Suaeda vera, a succulent halophyte endemic to hypersaline soils, has a promising role in enhancing the ecological resilience and phytoremediation of salinized lands. This study evaluated nine natural populations of *S. vera* from diverse habitats with varying salinity levels (ECe 1.77–39.75 dS m⁻¹) to assess key morphological, physiological and anatomical traits associated with salt tolerance. Sixteen plants per population were collected. Populations from the saline desert (SD), waterlogged (SW) and inundated (SI) areas exhibited enhanced growth and biomass under high salinity. These three populations accumulated elevated Na⁺ (roots: 107.1–125.80 mg g⁻¹; shoots: 116.40–146.60 mg g⁻¹) and Cl⁻ (roots: 53.71–65.90 mg g⁻¹; shoots: 58.9–73.1 mg g⁻¹), supporting osmotic regulation. Ion accumulation was complemented by high levels of organic osmolytes, including amino acids (up to 2905 µg g⁻¹ FW) and proline (50.9 µmol g⁻¹ FW). Salt-tolerant populations also showed elevated photosynthetic pigments (Chl a: 2.53, Chl b: 1.67, total Chl: 4.21, carotenoids: 0.09 mg g⁻¹ FW) and antioxidative enzyme activities (SOD: 27.7, POD: 37.6, catalase: 12.5 units mg g⁻¹ protein), contributing to stress mitigation. Anatomical adaptations included reduced/disintegrated cortical tissues, intense root (up to 1232.7 µm) and shoot sclerification (up to 425.1 µm), and thickened lamina (up to 954.1 µm) with enlarged spongy parenchyma, enhancing water storage (succulence up to 4.65 g water g⁻¹ DW). A high shoot bioconcentration factor (up to 1.69) indicated efficient accumulation/vacuolar sequestration of salts, supporting ion homeostasis. These traits highlight the phytoremediation potential of SD, SW, and SI populations, making *S. vera* a strong candidate for the reclamation of saline and degraded soils.

1. Introduction

Salinization has become a major threat to global land resources, affecting over one billion hectares of land across 100 countries, and this threat is expected to be exacerbated further with climatic change (Shi et al., 2023; Gautam et al., 2024). As a global ecological challenge, salinity stress places the vegetation of natural plant communities, agricultural productivity and food security at risk (Hossain, 2019; Safdar et al., 2019). Salt stress impairs plant growth by interfering with developmental, cellular, metabolic and molecular functions at both the

tissue and whole-plant levels (Sarwar et al., 2022). Elevated salt concentrations in soils and water create competition for ion absorption and disrupt the osmotic and ionic balance within plants, leading to physiological stress (Roy et al., 2014; Alam et al., 2019). This ionic imbalance, particularly the toxicity of Na⁺ and Cl⁻, impairs essential physiological and biochemical processes, notably photosynthesis (Rahneshan et al., 2018). The excessive accumulation of ions under saline conditions reduces the diffusion of carbon dioxide (CO₂) in leaves, alters metabolic pathways, and damages biomolecules such as proteins and DNA, resulting in oxidative stress in various cellular compartments (Bistgani

* Corresponding author.

E-mail addresses: nailaasghar123@gmail.com (N. Asghar), liuzhdy@163.com (Z. Liu), amnaameer127@gmail.com (A. Ameer), ahmadks@upr.edu.pk (K.S. Ahmad), ummar.iqbal@iub.edu.pk (U. Iqbal), hameedmansoor@yahoo.com (M. Hameed), shenying926@126.com (Y. Shen), hongxiangz86@163.com (Z. Hongxiang), kaleemkmal5798@gmail.com (M. Kaleem), ningty@163.com (T. Ning).

et al., 2019; Liu et al., 2020). These physiochemical changes adversely affect crop growth and productivity while limiting the diversity and spatial distribution of plant species in saline areas (Zörb et al., 2019).

Plants' adaptations to specific environments are crucial for survival in natural communities and provide unique opportunities to explore the mechanistic basis of adaptation through structural and functional analyses (Ahmad et al., 2019). However, quantifying the mechanisms of salt tolerance is challenging because of the complex nature of salt stress and the diverse responses of plants (Akhtar et al., 2017). Plants growing in saline environments have developed intrinsic salt tolerance mechanisms, making them valuable models for studying these processes. Halophytes, in particular, can withstand high salinity levels (Ben Hamed et al., 2016a,b) and exhibit significant biochemical modifications. Their salt tolerance is associated primarily with ion homeostasis, which relies on two main mechanisms: selective ion uptake or restricted nutrient supply, and ionic compartmentalization at the cellular and whole-plant levels (Tang et al., 2015). In hyper-saline environments, many halophytic species sequester excess Na^+ ions into vacuoles, using it as an inexpensive osmoticum to balance the cytoplasmic osmotic potential and maintain shoot succulence. Additionally, the accumulation of organic osmolytes, such as proline, soluble sugars, and proteins, helps maintain turgor pressure (Muchate et al., 2016). The detoxification of reactive oxygen species (ROS) also plays a crucial role in enhancing salt stress tolerance in these plants (You and Chan, 2015; Bistgani et al., 2019).

Plants that successfully adapt to environmental changes exhibit a range of structural modifications that increase their survival under harsh conditions. Many anatomical traits respond significantly to environmental stressors and are thus valuable indicators of plant response (Naskar and Palit, 2015). Anatomical traits associated with salinity tolerance include a thick epidermis and extensive sclerification in the stellar region, which provides mechanical support to the parenchymatous core and minimizes water loss and broad metaxylem vessels. The development of mesophyll parenchyma for salt and water storage, increased succulence, and alterations in stomatal characteristics to mitigate direct sunlight exposure are also critical adaptations (Abd El-Maboud and Khalil, 2013; Parida et al., 2016). Consequently, populations exhibiting optimal anatomical and physiological adaptations are better equipped to survive in saline soils.

Suaeda vera (alkali seepweed) is a perennial, euhalophytic shrub with succulent leaves and serves as an indicator species of salt-affected habitats (Naz et al., 2022). It is adapted to a variety of environments, including semi-arid and hyper-arid saline regions, salt marshes, and coastal lagoons. *S. vera* is characterized as a salt-accumulating species, primarily because of the substantial accumulation of Na^+ and Cl^- in leaf vacuoles for osmotic regulation, resulting in increased succulence (Obgurn and Edwards, 2010).

S. vera has emerged as a promising halophyte species for the phytoremediation of saline soils, offering a sustainable solution for restoring degraded and salt-affected agricultural lands. Its ecological role in mitigating soil salinity and enhancing soil health is well-recognized. However, the mechanisms by which different populations of *S. vera* adapt to and survive in hypersaline environments remain poorly understood. We hypothesize that distinct populations of *S. vera* subjected to varying degrees and durations of salinity stress have developed unique anatomical structures and physiological-biochemical traits that confer differential salt tolerance and survival capacity. The primary objectives of this study are 1) to characterize and compare the anatomical adaptations of *S. vera* populations originating from diverse saline habitats, 2) to quantify key physiological and biochemical parameters associated with salt stress tolerance, such as succulence, osmolyte accumulation, antioxidant enzyme activities, and ion homeostasis, and 3) to integrate these findings to identify trait patterns that underlie successful adaptation to hypersaline conditions. By achieving these objectives, this study aims to deepen our understanding of the adaptive strategies of *S. vera* and provide valuable insights for

optimizing its use in the phytoremediation and sustainable management of saline soils.

2. Materials and methods

2.1. Study area

Populations of *Suaeda vera* Forrsk. ex J.F. Gmel along with soil samples, were collected from nine ecologically distinct saline habitats across Punjab Province, Pakistan. These habitats were selected on the basis of the widespread distribution of this species (at least 20 plants per 500 m^2) and the salinity gradient ranged from high to low i) saline desert (SD), ii) saline waterlogged area (SW), iii) saline inundations (SI), iv) coarse sand desert (CS), v) dryland salinity (DS), vi) thal desert-margins, vii) cholistan desert-margins (CD), viii) sand dune desert (DD), and ix) roadside (RD). The map of the study habitats was derived using ArcGIS Pro-2.4.3 (Fig. 1). The climate data and soil physico-chemical characteristics of all the sampling sites are presented in Tables 1 and 2.

2.2. Soil samples

The soil in the root rhizosphere (15–25 cm deep) of each population ($n = 16$) was collected from each habitat and evaluated for physico-chemical properties according to the methodology outlined in Handbook # 60 (US Salinity Laboratory Staff, 1954). A saturation paste (1:2 by volume) was prepared from 200 g of air-dried soil samples to assess the soil pH, electrical conductivity (ECe), saturation percentage, and ionic content. Gradually, distilled water was added to the soil and mixed thoroughly until a uniform saturated paste was achieved. Subsequently, saturation-paste extract samples were obtained under partial vacuum at 2–4 atm. The saturation percentage was calculated by subtracting the dry weight of the soil from the weight of the saturated paste. The soil pH and electrical conductivity (ECe) were measured using a pH/ECe meter (WTW series, compact Ino LAB pH/Cond 720, Washington, USA) with the saturated-paste extract. Sodium (Na^+) and potassium (K^+) concentrations in the soil samples were quantified using a flame photometer (Jenway, PFP-7, UK). The calcium (Ca^{2+}) content was analyzed with an atomic absorption spectrophotometer (Model Analyst 3000: PerkinElmer, NW, CT), while the chloride ions (Cl^-) were examined using a digital chloride ion meter (Model-926, Sherwood Scientific Limited

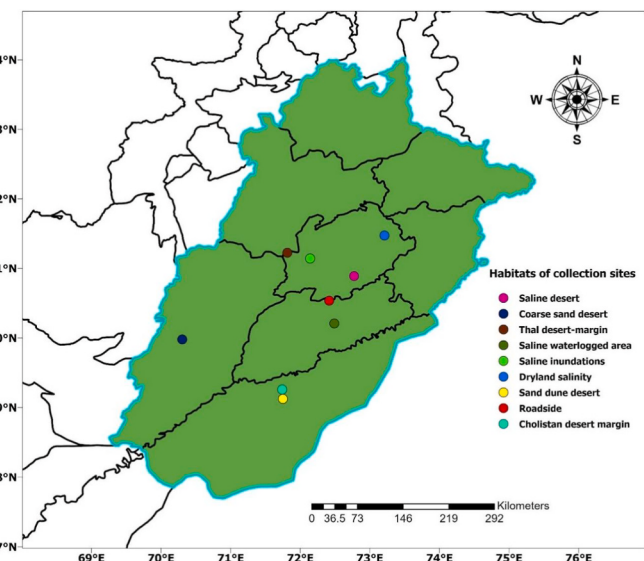


Fig. 1. Geographical distribution of *Suaeda vera* populations sampled from different saline habitats Punjab, Pakistan. Collection sites are indicated by color coded dots inside the map. Habitats names are listed on right side.

Table 1Metrological records of *Suaeda vera* populations collected from variously salt-affected habitats.

Ecological Habitats	Elevation (m a.s.l.)	Average rainfall (mm)	Average Summer temperature °C	Average Winter temperature °C	Coordinates		Habitats description/Environment type
					Latitude	Longitude	
SD	117	98.9	46.5	9.2	30°53'26.5" N	72°64'24.6" E	Hypersaline desert in Ladam sir
SW	144	226	42.2	7.3	30°16'05.21" N	71°55'55.29" E	Saline waterlogged area
SI	150	350	39.1	6.8	31°8'40.18" N	72°8'42.31" E	Saline inundations near Treemu Head works
CS	120	121	44.5	8.5	35°55'44.08" N	70°56'31.78" E	Coarse sandy desert in Rahim yar khan
DS	144	167	43.7	9.8	30°20'13.39" N	70°2'38.6" E	Saline arid zones near artifical forest plantation
TD	146	195	45.4	10.5	35°55'44.08" N	70°56'31.71" E	Margins of Thal desert
CD	92.2	143	52.5	13.9	28°24'58.59" N	70°51'50.38" E	Margins of Cholistan desert
DD	130	100	43.1	7.8	30°7'32.53" N	71°45'07.77" E	Hot arid region characterized by sand dune desert
RD	90	140	42.2	6.4	28° 37' 46.32" N	70° 37' 51.72" E	Extremely dry area along roadside

Ecological Habitats: SD: Saline desert; SW: Saline waterlogged area; SI: Saline inundations; CS: Coarse sand desert; DS: Dryland salinity; TD: Thal desert margin; CD: Cholistan desert margin; DD: Sand dune desert; RD: Roadside.

Table 2Soil physico-chemical characteristics of *Suaeda vera* populations collected from various salt-affected habitats.

Ecological Habitats	Soil texture	pH	ECe (dsm ⁻¹)	Na ⁺ (mg kg ⁻¹)	Cl ⁻ (mg kg ⁻¹)	Ca ²⁺ (mg kg ⁻¹)	K ⁺ (mg kg ⁻¹)	NO ₃ ⁻ (mg kg ⁻¹)	PO ₄ ³⁻ (mg kg ⁻¹)	OM (%)	SP (%)
SD	Sandy	8.5 ± 0.72 ^a	39.75 ± 3.80 ^a	5524.4 ± 33.93 ^a	3262.6 ± 29.44 ^a	52.2 ± 2.66 ^g	76.3 ± 3.71 ^h	2.7 ± 0.31 ^e	2.5 ± 0.25 ^g	0.88 ± 0.05 ^c	33 ± 3.02 ^{ab}
	clay	8.2 ± 0.59 ^b	32.36 ± 2.95 ^b	4777.2 ± 31.09 ^b	2517.9 ± 27.34 ^b	51.5 ± 2.18 ^g	75.8 ± 3.66 ^h	2.5 ± 0.22 ^f	5.4 ± 0.54 ^d	0.78 ± 0.04 ^f	33 ± 3.12 ^{ab}
SW	Loamy to clayey	8.2 ± 0.59 ^b	32.36 ± 2.95 ^b	4777.2 ± 31.09 ^b	2517.9 ± 27.34 ^b	51.5 ± 2.18 ^g	75.8 ± 3.66 ^h	2.5 ± 0.22 ^f	5.4 ± 0.54 ^d	0.78 ± 0.04 ^f	33 ± 3.12 ^{ab}
	loamy	8.2 ± 0.62 ^b	26.43 ± 2.88 ^c	3608.9 ± 29.98 ^c	1781.6 ± 26.81 ^c	66.7 ± 2.43 ^f	98.4 ± 4.13 ^g	2.4 ± 0.21 ^f	2.7 ± 0.27 ^f	0.80 ± 0.05 ^e	35 ± 2.66 ^a
SI	Sandy	7.5 ± 0.56 ^c	18.59 ± 1.55 ^d	2719.3 ± 26.71 ^d	1358.8 ± 23.18 ^d	69.4 ± 2.74 ^e	180.4 ± 5.91 ^d	2.9 ± 0.47 ^d	9.6 ± 0.91 ^a	0.95 ± 0.06 ^{ab}	32 ± 2.45 ^b
	loam	8.2 ± 0.61 ^b	12.07 ± 1.58 ^f	1560.7 ± 21.69 ^f	786.8 ± 13.76 ^f	107.5 ± 3.98 ^c	261.2 ± 6.31 ^c	2.7 ± 0.24 ^e	8.3 ± 0.68 ^c	0.83 ± 0.04 ^d	30 ± 1.57 ^c
CS	Sandy	7.6 ± 0.51 ^c	15.78 ± 1.34 ^e	2517.3 ± 26.94 ^e	1258.7 ± 16.49 ^e	88.9 ± 3.01 ^d	167.4 ± 5.29 ^f	2.8 ± 0.41 ^{de}	9.8 ± 0.96 ^b	0.93 ± 0.06 ^b	31 ± 1.99 ^{bc}
	loam	8.2 ± 0.61 ^b	12.07 ± 1.58 ^f	1560.7 ± 21.69 ^f	786.8 ± 13.76 ^f	107.5 ± 3.98 ^c	261.2 ± 6.31 ^c	2.7 ± 0.24 ^e	8.3 ± 0.68 ^c	0.83 ± 0.04 ^d	30 ± 1.57 ^c
DS	Sandy	8.3 ± 0.81 ^b	10.27 ± 0.95 ^g	1085.5 ± 18.63 ^g	496.6 ± 8.74 ^g	127.4 ± 4.32 ^b	174.01 ± 5.15 ^e	3.8 ± 0.52 ^b	4.2 ± 0.46 ^e	0.64 ± 0.03 ^g	32 ± 2.46 ^b
	loam	8.5 ± 0.91 ^a	8.54 ± 0.84 ^h	859.9 ± 14.91 ^h	399.2 ± 7.61 ^h	128.8 ± 5.13b	390.3 ± 7.97 ^a	3.1 ± 0.51 ^c	8.4 ± 0.77 ^c	0.99 ± 0.06 ^a	31 ± 2.08 ^{bc}
TD	Sandy	8.2 ± 0.61 ^b	1.77 ± 0.11 ⁱ	188.9 ± 5.01 ⁱ	94 ± 3.43 ⁱ	144.6 ± 5.91 ^a	353.5 ± 7.54 ^b	7.7 ± 0.89 ^a	0.89 ± 0.05 ^h	0.79 ± 0.04 ^f	35 ± 3.55 ^a
	loam	8.2 ± 0.61 ^b	1.77 ± 0.11 ⁱ	188.9 ± 5.01 ⁱ	94 ± 3.43 ⁱ	144.6 ± 5.91 ^a	353.5 ± 7.54 ^b	7.7 ± 0.89 ^a	0.89 ± 0.05 ^h	0.79 ± 0.04 ^f	35 ± 3.55 ^a
F-ratio		34.56	3360.32	5583.85	10,747.11	11,727.81	455,447.20	2490.50	11,509.50	1013.44	14.64
P value		<0.001***	<0.001***	<0.001***	<0.001***	<0.001***	<0.001***	<0.001***	<0.001***	<0.001***	<0.001***

Means ± SE (n = 16); Means sharing different letters indicate significant differences at P ≤ 0.05 (LSD), *** significance at P ≤ 0.001.

Ecological Habitats: SD: Saline desert; SW: Saline waterlogged area; SI: Saline inundations; CS: Coarse sand desert; DS: Dryland salinity; TD: Thal desert margin; CD: Cholistan desert margin; DD: Sand dune desert; RD: Roadside.

Soil physico-chemical characteristics: pH: hydrogen ion concentration; ECe: electrical conductivity; Na⁺: soil sodium; Cl⁻: soil chloride; K⁺: soil potassium; Ca²⁺: soil calcium; NO₃⁻: soil nitrate; PO₄³⁻: soil phosphate; OM: organic matter; SP: saturation percentage.

Cambridge, UK). The soil phosphate (PO₄³⁻) and nitrate (NO₃⁻) contents were determined by the methods described by [Yoshida et al. \(1976\)](#) and [Kowalenko and Lowe \(1973\)](#), respectively, while soil organic matter was evaluated using the methodology described by Walkley-Black ([Jackson, 1962](#)).

2.3. Plant sampling

Nine distinct populations of *S. vera* were selected from nine geographically and environmentally diverse habitats across the study region. These sites were chosen on the basis of documented gradients of soil salinity levels to capture a representative range of saline conditions, as detailed in the Study area section. This stratified sampling design aimed to encompass spatial heterogeneity and ecological variability within the species' natural distribution. In each habitat, sixteen average-sized, mature plants were randomly sampled to ensure adequate representation of intra-population variation and minimize sampling bias. The total sample size of 144 plants (n = 16 × 9) balances logistical

feasibility with statistical robustness for morpho-anatomical and physiological analyses. The sampling plots within each habitat were systematically distributed to reflect microhabitat variability and to avoid spatial clustering. GPS coordinates were recorded for each sampled plant to accurately map geographical distribution and enable spatial analyses of trait variation in relation to environmental factors. The plants were carefully excavated using a 15 cm diameter soil auger to collect entire intact root systems, preserving the belowground structures critical for anatomical studies. The samples were gently washed in situ to remove adhering soil and plant debris without compromising tissue integrity. Fresh weights were immediately recorded with a digital top-loading balance to reduce post-harvest water loss bias. To maintain sample quality, individual plants were sealed in labeled plastic zip-lock bags (24 × 14 cm) and transported in insulated coolers to the laboratory for further morphological, anatomical, and physiological assessments. This comprehensive sampling strategy, which combines purposive site selection, randomized plant selection within stratified plots, and precise georeferencing, was designed to maximize the representativeness of

S. vera populations across environmental gradients and to support robust inference about their adaptive traits.

2.4. Morphological characteristics

To determine their morphological traits, the plants were carefully uprooted and washed with tap water to remove soil particles. To determine the fresh weight, the uprooted plants were weighed immediately using a portable digital scale. These uprooted plants were transported to the laboratory, where root and shoot lengths were measured using a meter rod. For dry weight, the samples were then oven-dried at 70 °C for 72 h until a constant weight was reached. The fresh and dry weights were used to calculate the plant water contents using the following formula:

$$\text{Plant water contents(g plant)} = \frac{\text{Fresh weight of the plant (g plant)}}{\text{oven dried weight (g plant)}}$$

$$\text{Succulence (g water g plant}^{-1} \text{DW}) = \frac{\text{FW} - \text{DW}}{\text{DW}}$$

The leaf area was calculated by using the following formula: (length × width × correction factor 0.75)

2.5. Physiological characteristics

2.5.1. Plant ionic contents

To estimate the tissue ionic contents of the plants, oven-dried plant material (roots and leaves) was ground into powder with a mortar and pestle. In a digestion flask, 0.5 g of dry material from each sample was acid digested with 5 mL of concentrated H₂SO₄ using the Wolf (1982) method. After incubation for 24 h, the digestion flasks were transferred to a hot plate, and 0.5 mL of 30 % H₂O₂ (v/v) was added at 100 °C. The temperature gradually increased to 380 °C until the fumes dissipated. After cooling, 0.5 % H₂O₂ was added, and the mixture was re-heated again to 380 °C. This process was repeated several times until the plant material became completely decolorized. After digestion, the mixture was diluted with distilled water to 50 mL and filtered. Finally, the filtrate was stored at 4 °C for the analyses Na⁺, K and Ca²⁺ ions using a flame photometer (PFP-7, Jenway, UK). For chloride (Cl⁻) ions, 0.1 g of root and/or shoot samples were ground and digested with 10 mL of distilled water at 80 °C until the volume reached half the original value (Tavakkoli et al. 2010). Following cooling, the final volume was brought to 10 mL again by adding distilled water. Cl⁻ ions were measured using a chloride meter (Sherwood Model-926, Cambridge, UK).

2.5.2. Photosynthetic pigments

Fresh leaf samples (0.2 g) were extracted overnight with 80 % cold acetone (10 mL), ground and homogenized to access the chlorophyll *a* and *b* (Chl *a* and *b*) Arnon (1949) and carotenoids using the Davis method (1977). The homogenized plant extract was then centrifuged at 10,000×g for 5 min. The absorbance of the supernatant was determined at various wavelengths (480, 645, and 663 nm) using a UV-visible spectrophotometer (Model, Hitachi-220, Japan).

2.5.3. Compatible solutes

To determine the total free amino acid contents, 1 g of fresh leaf material was extracted in 10 mL of citrate buffer (pH 5.5) using the method outlined by Moore and Stein (1948). The extracted material was incubated at room temperature for 60 min and then centrifuged at 15,000 rpm for 10 min at 15 °C. Then, 1.0 mL of the supernatant was transferred to test tubes and mixed with 1.0 mL of ninhydrin solution. The test tubes were covered with aluminum foil, heated in a boiling water bath for 20 min and cooled. The reaction mixture was then diluted with 5 mL of n-propanol and H₂O (1:1 ratio) and incubated for 15 min at room temperature. The OD was measured at 530 nm using a

spectrophotometer (Hitachi, 220, Tokyo, Japan).

The free proline contents were calculated using a protocol established by Bates et al. (1973). For this purpose, 0.5 g of fresh leaf material was homogenized with 2 mL sulfosalicylic acid (3%). After filtration, ninhydrin solution (2 mL) and glacial acetic acid (2 mL) were added to the 2 mL of sample extract. The reaction mixture was heated at 100 °C in a water bath for half an hour. After cooling in an ice bath, each sample was treated with 4 mL of toluene. Following agitation, the absorbance of the extracted samples was measured at 520 nm using a double beam spectrophotometer (Hitachi, 220, Tokyo, Japan). For proline estimation, a graded series of proline (10–100 ppm) was used to generate a standard curve.

To estimate the total soluble protein content, fresh leaf material (0.25 g) was chopped in 5 mL of potassium phosphate buffer (50 mM, pH 7.7). The chopped leaf material was then subjected to centrifugation at 12,000 rpm, for 15 min and the resulting supernatant was collected for analysis. One hundred milliliters of supernatant from each sample and Bradford reagent (2 mL) were added to the vessels, which were then vortexed for 10 s. The absorbance of the mixture was measured using a spectrophotometer (Hitachi, 220, Japan) at 595 nm.

For analyses of total soluble sugars, 0.1 g of dried leaf material was extracted with 80 % ethanol solution. The extracted material was incubated at 60 °C for 6 h, followed by centrifugation at 15,000 rpm for 15 min. The aliquot (0.1 mL) was added to 3 mL of anthrone reagent and heated at 60 °C for 30 min. Following 20 min of incubation at 25 °C, the reaction mixture was cooled in ice cubes. The absorbance was observed at 625 nm on a spectrophotometer (Hitachi, 220, Tokyo, Japan). A standard curve was constructed using serial dilution of glucose to quantify total soluble sugars (Yemm and Willis, 1954).

2.5.4. Enzymatic antioxidants

Fresh leaf samples (0.5 g) were homogenized in 5 mL of ice-cooled potassium phosphate buffer (50 mM) using pre-chilled pestle and mortar. The extracted plant material was subsequently transferred to centrifuge tubes and centrifuged for approximately 20 min at 20,000×g. The separated supernatant was then stored at –20 °C and used for the measurement of enzymatic activities such as those of superoxide dismutase, catalase and peroxidase. The activity of SOD (superoxide dismutase) in leaves is based on the principle of inhibition of nitroblue tetrazolium (NBT) photoreduction (Giannopolitis and Ries, 1977), whereas the activities of catalase (CAT) and peroxidase (POD) are assayed following the methods of Chance and Maehly (1955). For the determination of the activity of the CAT enzyme, 0.1 mL of supernatant, 1.9 mL of potassium phosphate buffer and 1 mL of H₂O₂ (45 mM) were mixed in a cuvette. The changes in absorbance of the reaction mixture were noted at 470 nm with intervals of 30 s up to 120 s via a spectrophotometer (Hitachi, 220, Japan).

To determine POD (peroxidase) activity, mixtures of 750 μL of potassium phosphate buffer (50 mM), 750 μL hydrogen per oxide (40 mM), 100 μL guaiacol (20 mM) and 0.1 mL of enzyme extract were mixed in test tubes. The absorbance of each sample was measured at 470 nm every 20 s for 2 min.

2.6. Phytoremediation traits

The bioconcentration factor (BCF), translocation factor (TF), and dilution factor (DF) for sodium (Na⁺) and chloride (Cl⁻) were determined by the formula devised by Diwan et al. (2010).

$$BCF = \frac{\text{Concentration of sodium and chloride in plant tissue (mg/g)}}{\text{Concentration of sodium and chloride in soil (mg/kg)}}$$

$$TF = \frac{\text{sodium and chloride ions in leaves (mg/g DW)}}{\text{sodium and chloride ions in root (mg/g DW)}}$$

$$DF = (BCF \text{ root or shoot}) \times (\text{dry weight of root or shoot (g)} \times 100)$$

2.7. Anatomical characteristics

For anatomical measurements, fully expanded leaves, tallest stems and 2 cm sections of the thickest tap root were separated from the plant body. The selected plant material was immediately fixed in formalin-acetic alcohol fixative composed of 10 % formaldehyde, 5 % acetic acid, 50 % ethyl alcohol, and 35 % distilled water for 48 h. Thereafter, the samples were subsequently transferred to acetic-alcohol solution including (25 % acetic acid and 75 % ethanol) for prolonged storage. Permanent slides of plant tissues were made using freehand sectioning technique. Thin transverse sections were then carefully separated in Petri dishes and gradually dehydrated using a series of ethyl alcohol solution (30–100 %). To create contrast, the double staining method was followed using safranin for lignified tissues and fast green for primary tissues. Following dehydration, the samples were cleared with xylene and mounted on glass slides using Canada balsam. Anatomical measurements (magnification = 40 \times) of different cells and tissues were noted by using pre-calibrated ocular micrometer. Microphotographs were captured with a camera equipped with a microscope (Nikon 104, Tokyo, Japan).

2.8. Statistical analysis

The experiment was designed in a completely randomized design (CRD). The data were subjected to analysis of variance (ANOVA) by using Minitab statistical software (version 19). The least significant difference (LSD) test at the significance level ($P < 0.05$) was employed to compare the mean differences among populations. The graphs and data visualization were generated using Origin Pro (version 2019b, 9.65) by Origin Lab Corporation. The correlation matrix and heatmap were used to evaluate the relationships between morpho-physiological and anatomical attributes using customized codes ('pheatmap' and 'GGally' packages) in R Studio 1.1.463.

3. Results

3.1. Soil physicochemical characteristics

Sandy loam soil was predominant in most of the habitats where the populations were collected. In contrast, sandy clay was found in the saline desert, loamy to clay loamy soils were observed in the saline waterlogged areas, and loamy sand was present in the saline inundations (Table 2). The soil pH across all habitats was alkaline, ranging from 7.5 to 8.5. The lowest pH (7.5) was recorded in the soil from the coarse sand desert, while the highest pH (8.5) was found in the soils from both the saline desert and the sand dune desert. The soil EC ranged from 1.77 to 39.75 dsm⁻¹, the soil Na⁺ concentration ranged from 188.9 to 5524.4 mg kg⁻¹ and Cl⁻ ranged from 94 to 3662.6 mg kg⁻¹, with the highest value occurring in the saline desert and the lowest value occurring at the roadside. The highest soil Ca²⁺ concentration (144.6 mg kg⁻¹) was recorded on the roadside, while the lowest was noted in the saline waterlogged area. The soil K⁺ concentration reached a maximum of 390.3 mg kg⁻¹ in the sand dune desert, but the lowest concentration was in the saline waterlogged area. The habitats of the Cholistan desert margin and roadside area presented the highest soil NO³⁻ content (3.8 mg kg⁻¹), while the soil associated with saline inundations had the lowest 2.4 mg kg⁻¹. In dryland salinity, the maximum soil PO₄³⁻ concentration of 9.8 mg kg⁻¹ was recorded, while the minimum PO₄³⁻ concentration of 0.89 mg kg⁻¹ was recorded at the roadside. In the soil of the sand dune desert, the organic matter content was the highest at 0.99 %, whereas lowest value of 0.64 % was noted in the soil collected from the Cholistan desert margin. The soil saturation percentage ranged from 30 % in the Thal desert margin to 35 % in the saline inundation and roadsides (Table 2).

3.2. Morphological characteristics/growth attributes

In all the habitats, the growth attributes of *S. vera* populations differ (Fig. 2). The root length increased significantly with increasing salinity level in the studied habitats. The root length increased markedly (112 cm plant⁻¹) in the population in the saline desert habitat, whereas it decreased significantly (19.67 cm plant⁻¹) in the roadside population. The plants growing in the saline waterlogged area had the maximum shoot length (96.12 cm plant⁻¹) and leaf area (0.78 cm² leaf⁻¹), while those from the roadside had shorter shoots (15.67 cm plant⁻¹) with smaller leaves (0.11 cm² leaf⁻¹). The root and shoot fresh and dry weights of the *S. vera* plants exhibited similar trends across all the habitats. Populations from the saline waterlogged area had significantly greater fresh weights (37.01 g plant⁻¹, 46.67 g plant⁻¹) and dry weights (6.80 g plant⁻¹, 46.67 g plant⁻¹), while roadside populations had the lowest fresh and dry weights (3.20 g plant⁻¹, 4.33 g plant⁻¹ and 1.14 g plant⁻¹, 0.96 g plant⁻¹). The root water content showed a pattern of increase similar to that observed for the fresh and dry weights, whereas shoot water content was highest in populations from three the habitats i.e., the saline waterlogged area, saline inundations and saline desert, at 38.63, 31.2 and 30.7 g plant⁻¹, respectively. Succulence exhibited significant variations across all habitats, with the highest (4.65, 31.2 and 4.57 g water g⁻¹ plant DW) recorded in the saline waterlogged area and saline inundation populations, closely followed by the saline desert, coarse sand desert and dryland salinity populations (Fig. 2).

3.3. Physiological traits

3.3.1. Tissue ionic contents

The Na⁺ and Cl⁻ contents in both the roots and shoots increased significantly along the increasing salinity gradient in the studied habitats (Fig. 3). However, the accumulation of Na⁺ in roots and shoots was significantly greater (125.80 mg g⁻¹ DW, 146.60 mg g⁻¹ DW) in saline desert populations than in their counterparts from all habitats. The root and shoot Cl⁻ contents followed a similar pattern as the sodium concentration and reached a maximum (65.90 mg g⁻¹ DW and 73.10 mg g⁻¹ DW, respectively) in the saline desert population. The root and shoot K⁺ concentrations decreased substantially with increasing salinity level of habitats. Root K⁺ was highest (52.11 mg g⁻¹ DW) in populations collected from Thal-desert margin and lowest (24.01 and 25.26 mg g⁻¹ DW) in two populations collected from the saline desert and roadside. Conversely, shoot K⁺ was highest (38.19 mg g⁻¹ DW) in the coarse sand desert and lowest (17.55 and 18.05 mg g⁻¹ DW) in the saline desert and roadside areas, respectively. The root and shoot Ca²⁺ contents were significantly higher (13.73 and 21.68 mg g⁻¹ DW) in the saline waterlogged areas, while the roadside populations had the lowest root Ca²⁺ content (7.63 mg g⁻¹ DW), and the roadside and sand dune desert populations had the lowest shoot content (7.58 and 7.68 mg g⁻¹ DW, respectively) (Fig. 3).

3.3.2. Photosynthetic pigments

Populations from saline waterlogged areas and saline inundations exhibited significantly higher levels of chlorophyll *a*, with values reaching 2.53 mg g⁻¹ FW, while roadside populations had the lowest concentration at 0.64 mg g⁻¹ FW (Fig. 3). The highest levels of chlorophyll *b* (1.67 and 1.56 mg g⁻¹ FW) and total chlorophyll (4.21 and 3.83 mg g⁻¹ FW) were recorded in the saline waterlogged and saline desert populations, respectively. In contrast, the lowest chlorophyll *b* and total chlorophyll levels (0.42 and 1.05 mg g⁻¹ FW, respectively) were detected in the roadside populations. The carotenoid content was also highest in the plants from the saline desert (0.09 mg g⁻¹ FW) and the lowest in the roadside plants (0.01 mg g⁻¹ FW) (Fig. 3).

3.3.3. Organic osmolytes

The contents of compatible solutes, specifically amino acids and proline, significantly increased with increasing salinity levels in the

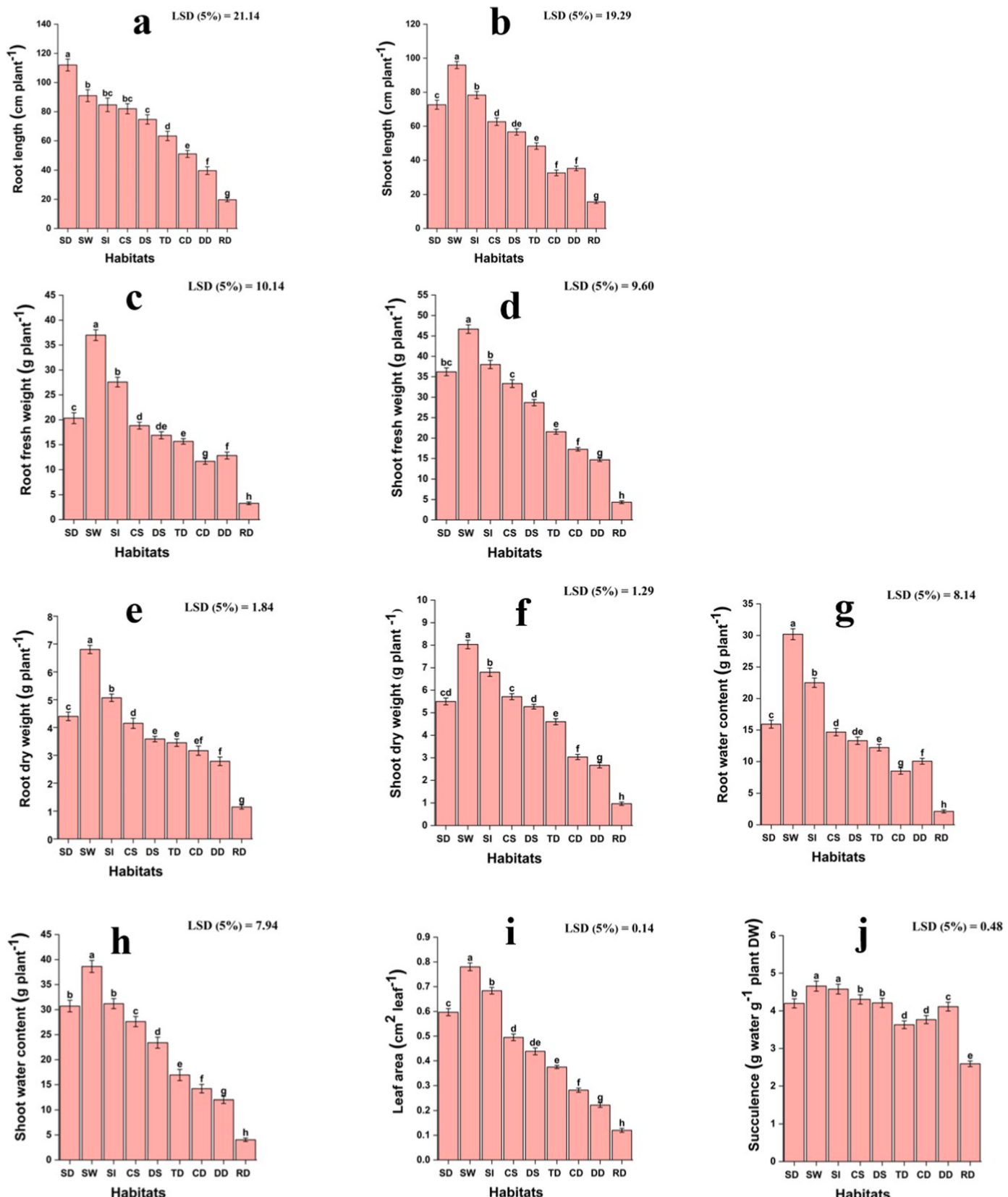


Fig. 2. Morphological attributes of *Suaeda vera* populations sampled from various salt-affected habitats. (a) Root length (b) Shoot length (c) Root fresh weight (d) Shoot fresh weight (e) Root dry weight (f) Shoot dry weight (g) Root water content (h) Shoot water content (i) Leaf area (j) Succulence. Means \pm SE ($n = 16$) are provided with error bars; different letters indicate significant differences at $P \leq 0.05$. Ecological Habitats: SD: Saline desert; SW: Saline waterlogged area; SI: Saline inundations; CS: Coarse sand desert; DS: Dryland salinity; TD: Thal desert margin; CD: Cholistan desert margin; DD: Sand dune desert; RD: Roadside.

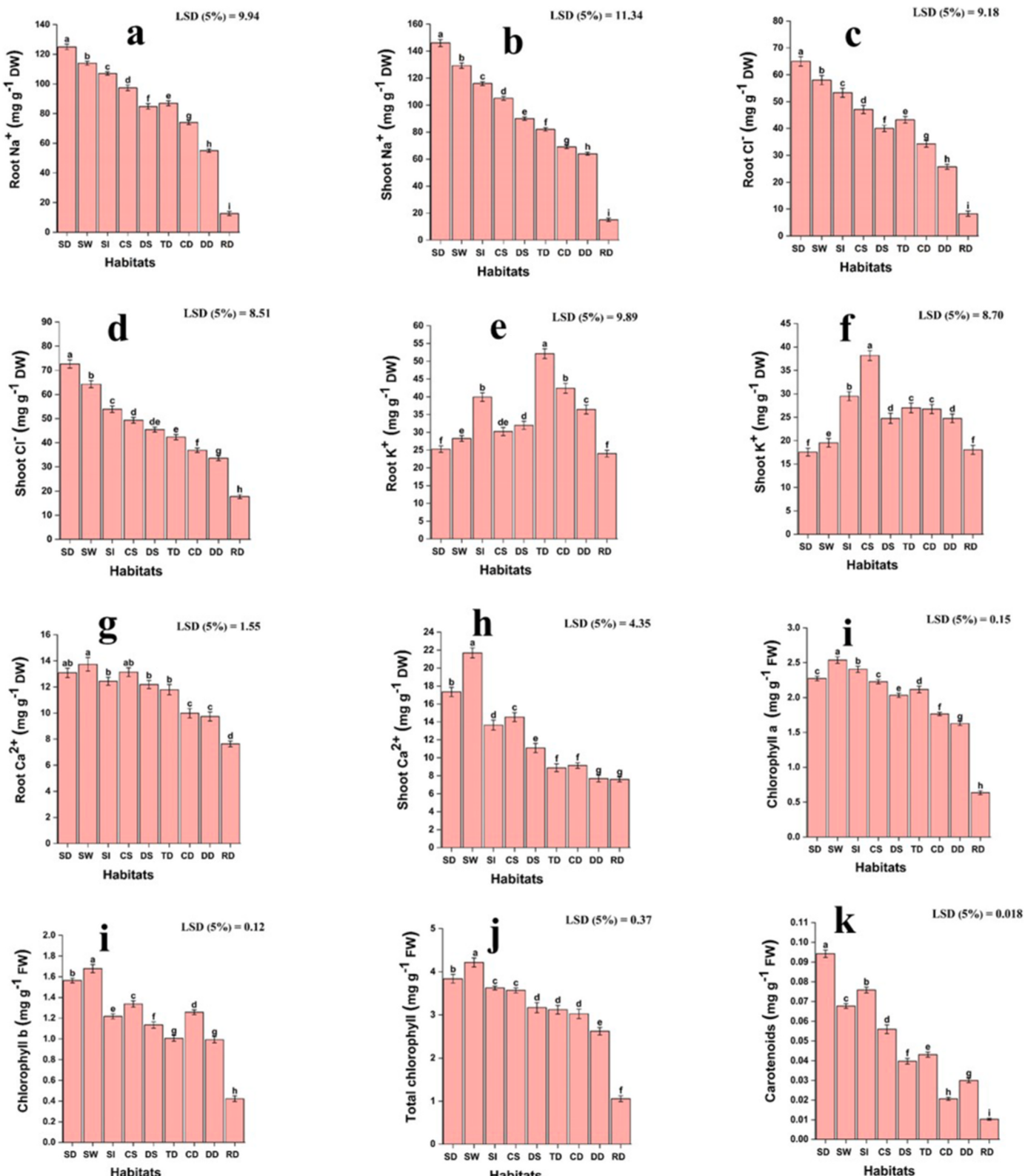


Fig. 3. Tissue ionic contents and photosynthetic pigments of *Suaeda vera* populations sampled from various salt-affected habitats. (a) Root Na⁺ (b) Shoot Na⁺ (c) Root Cl⁻ (d) Shoot Cl⁻ (e) Root K⁺ (f) Shoot K⁺ (g) Root Ca²⁺ (h) Shoot Ca²⁺ (i) Chlorophyll a (j) Chlorophyll b (k) Total chlorophyll (l) Carotenoids. Means \pm SE ($n = 16$) are provided with error bars; different letters indicate significant differences at $P \leq 0.05$. Ecological Habitats: SD: Saline desert; SW: Saline waterlogged area; SI: Saline inundations; CS: Coarse sand desert; DS: Dryland salinity; TD: Thal desert margin; CD: Cholistan desert margin; DD: Sand dune desert; RD: Roadside.

habitats (Fig. 4). Populations from the saline desert and saline waterlogged areas exhibited the highest concentrations of total free amino acids (2905.8 and 2679.2 $\mu\text{mol g}^{-1}$ FW, respectively) and proline (50.94 and 42.91 $\mu\text{mol g}^{-1}$ FW, respectively). In contrast, the roadside populations had the lowest values for these compounds, measuring only 116.5 and 4.2 $\mu\text{mol g}^{-1}$ FW. Conversely, the total soluble sugars and proteins decreased as the habitat salinity increased. The total soluble protein levels were highest in the coarse sand desert (35.7 mg g^{-1} DW) and dryland salinity populations (34.6 mg g^{-1} DW), while the roadside population recorded the lowest level at 6.04 mg g^{-1} DW. The maximum accumulation of total soluble sugars (42.5 mg g^{-1} DW) was found in the shoots of the dryland salinity population, whereas the roadside

population had the minimum accumulation at 7.8 mg g^{-1} DW (Fig. 4).

3.3.4. Enzymatic antioxidants

Catalase (CAT) activity was highest in the saline desert population, measuring 12.5 units mg g^{-1} protein, and tended to decrease with decreasing salinity, reaching its lowest level at 1.01 units mg g^{-1} protein in the roadside population (Fig. 4). The superoxide dismutase (SOD) activity followed a similar pattern, peaking at 27.6 units mg g^{-1} protein in the saline desert habitat, followed by 25.17 units mg g^{-1} proteins in the waterlogged area, and dropping to a minimum of 3.2 units mg g^{-1} proteins in the roadside populations. The population from the saline waterlogged area exhibited the highest peroxidase (POD) activity at

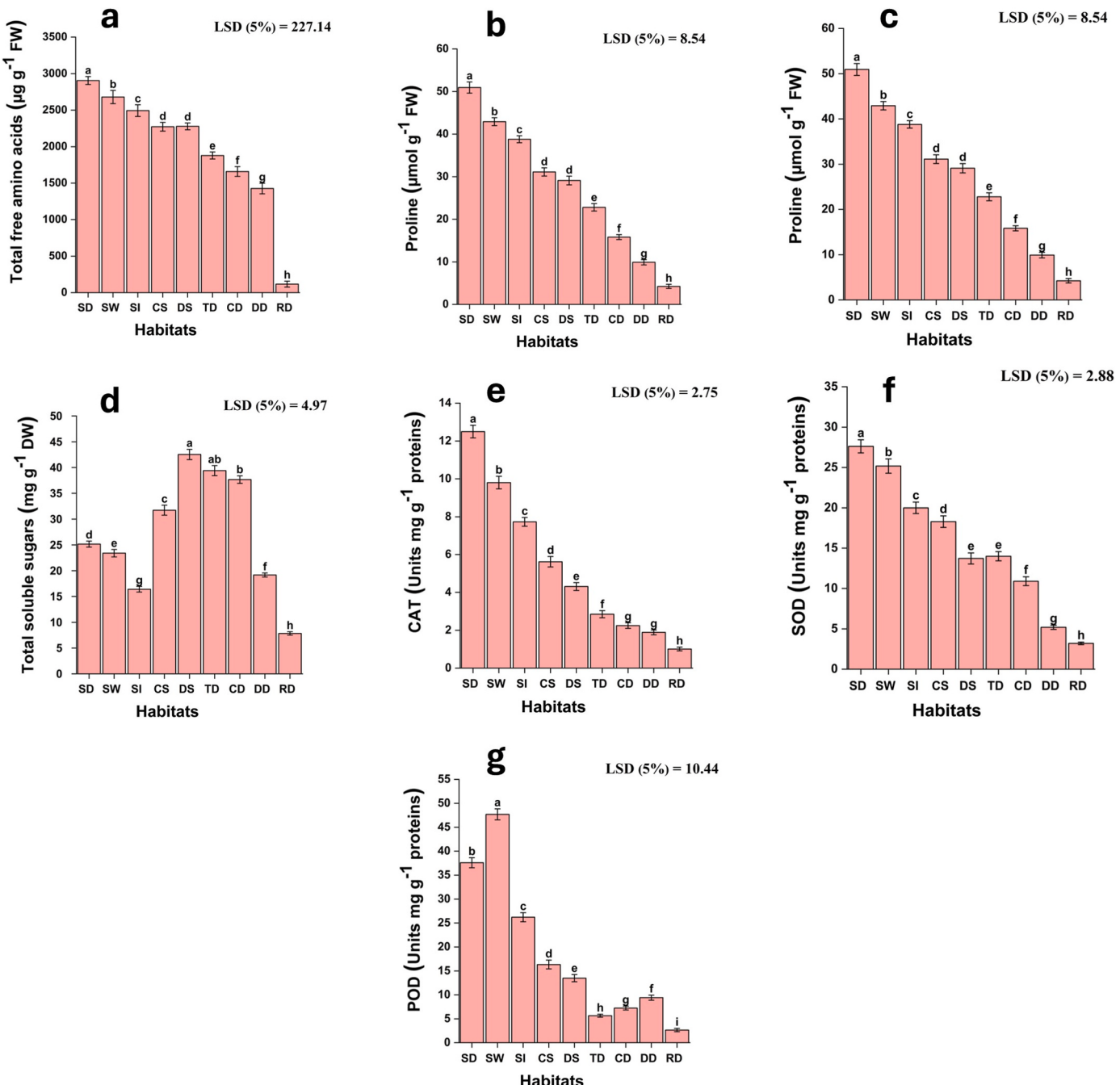


Fig. 4. Organic osmolytes and enzymatic antioxidants of *Suaeda vera* populations sampled from various salt-affected habitats. (a) Total free amino acids (b) proline (c) total soluble proteins (d) total soluble sugars (e) catalase (f) superoxide dismutase (g) peroxidases. Means \pm SE ($n = 16$) are provided with error bars; different letters indicate significant differences at $P \leq 0.05$. Ecological Habitats: SD: Saline desert; SW: Saline waterlogged area; SI: Saline inundations; CS: Coarse sand desert; DS: Dryland salinity; TD: Thal desert margin; CD: Cholistan desert margin; DD: Sand dune desert; RD: Roadside.

47.6 units mg g^{-1} protein, while the roadside and Thal desert margin populations had the lowest POD activities, measuring 2.6- and 5.6-units mg g^{-1} protein, respectively (Fig. 4).

3.4. Anatomical traits

3.4.1. Root anatomy

The root area was the attribute least affected by salt stress. However, in saline inundations and Cholistan desert margin populations, this attribute significantly increased and ranged from 0.92 to 0.98 mm^2 , whereas the dryland salinity population had the lowest value (0.60 mm^2) (Table 3, Fig. 5). Cortical thickness showed a decreasing trend as the salinity level of the habitats increased, but it was more pronounced in the dryland salinity populations and was measured as 33.03 μm . Disintegration of the cortical region was also observed in plants originating from highly saline habitats, such as saline desert and saline waterlogged areas. The cortical region was well-developed in the Cholistan desert margin (335.35 μm) and Thal desert margin populations (330.63 μm). The cortical cell area showed the same trend as was noted for cortical thickness. The broadest metaxylem vessels ($6941.5 \mu\text{m}^2$, $5889.8 \mu\text{m}^2$) were recorded in two populations from dryland salinity and saline desert, while the narrowest ($473.28 \mu\text{m}^2$) was recorded in the saline inundation population. The phloem area was reached a maximum ($6047.50 \mu\text{m}^2$) in the saline desert population and a minimum ($1893.15 \mu\text{m}^2$) in the population from the Thal desert margin. The area of the Stellar region was significantly greater (0.82–0.87 mm^2) for the plants collected from the saline waterlogged area and saline inundations. The stellar region was smaller (0.21–0.23 mm^2) for the two populations from Thal desert margin and roadside. In the case of sclerenchyma tissue thickness, the populations inhabiting, saline waterlogged areas, saline inundations and saline desert had maximum thickness (1048.58–1232.79 μm) of sclerenchyma tissue. Conversely, the lowest value for this parameter (429.82 μm) was noted in the Thal desert margin population (Table 3, Fig. 5).

3.4.2. Stem anatomy

The highest stem cross sectional area (1.32 mm^2), epidermis thickness (118.08 μm), epidermal cell area ($3365.6 \mu\text{m}^2$), cortex region thickness (406.2 μm) and cortical cell area ($10,307.6 \mu\text{m}^2$) were noted in the plants collected from saline inundations (Table 3, Fig. 6). In contrast, the plants collected from the roadside had the lowest values for the stem cross sectional area (0.79 mm^2), epidermis thickness (33.06 μm) and epidermal cell area ($525.87 \mu\text{m}^2$). The population from the dryland salinity had the smallest cortex region (99.19 μm), while the population from the saline desert had the smallest cortical cell area (1051.75 μm^2). Larger vascular bundles ($43,069.21 \mu\text{m}^2$), enlarged metaxylem vessels ($3313.01 \mu\text{m}^2$) and phloem area ($6100.15 \mu\text{m}^2$) were recorded in plants adapted to coarse sand desert. The plants collected from the Cholistan desert margin possessed smaller vascular bundles ($13,462.41 \mu\text{m}^2$), smaller metaxylem vessels ($368.11 \mu\text{m}^2$) and phloem region ($2734.55 \mu\text{m}^2$), whereas, the sand dune desert population also had the lowest value for metaxylem vessels and saline inundations population in the phloem region. The increasing salinity level of the habitats resulted in an increase in the stem sclerified bundle thickness and sclerenchyma region. Enlarged sclerified bundles ($89.74 \mu\text{m}^2$) and sclerenchyma regions ($425.10 \mu\text{m}$) were recorded in the saline desert population, but the lowest values for sclerified bundles ($47.23 \mu\text{m}^2$) were recorded in the Cholistan desert margin and for the sclerenchyma region (103.91, 108.63 μm) in the coarse sand desert and roadside. The highest proportion (987.17, 921.05 μm) of the pith region was noted in two populations from the saline desert and coarse sand desert and the largest pith cell area ($6310.51 \mu\text{m}^2$) was in the saline inundation population. In contrast, the populations collected from the margin of the Cholistan desert showed significant reductions in these traits (Table 3, Fig. 6).

3.4.3. Leaf anatomy

An increase in leaf lamina thickness was recorded with increasing salinity in the habitats. The plants from the saline waterlogged area had the thickest leaf lamina (954.11 μm), while those from roadside had the thinnest leaf lamina (377.86 μm) (Table 3, Fig. 7). The epidermal layer was thickest in the plants collected from saline desert and saline waterlogged areas, which ranged from 113.36 to 118.08 μm , whereas the thinnest epidermis (37.78 μm) was observed in the roadside plants. Populations collected from saline inundation and saline waterlogged areas had larger epidermal cell areas ($5944.98 \mu\text{m}^2$, $5942.39 \mu\text{m}^2$), while those collected from roadside areas had the smallest epidermal cell area ($2839.32 \mu\text{m}^2$). The saline waterlogged area population had the thickest palisade tissue at 146.42 μm , followed by the saline desert population at 122.81 μm .

The roadside population had the thinnest palisade mesophyll (51.95 μm). The proportion of spongy mesophyll was highest (552.63 μm) in the plants from saline waterlogged areas, followed by the plants from saline inundation (519.56 μm), and lowest (151.14 μm) in the roadside populations. In contrast, the spongy cell area was greatest (17879.77 μm^2) in the saline inundation population, followed by the saline desert population ($13,567.59 \mu\text{m}^2$), and it was lowest ($5259.59 \mu\text{m}^2$) in the roadside population. The total vascular bundle area ($27.94 \mu\text{m}^2$), xylem area ($5153.53 \mu\text{m}^2$) and phloem area ($4154.41 \mu\text{m}^2$) of the saline desert population surpassed those of the other habitats, whereas the total vascular bundle area ($10.17 \mu\text{m}^2$), xylem area ($1156.92 \mu\text{m}^2$) and phloem region ($1262.11 \mu\text{m}^2$) of the roadside population were the lowest. The stomatal density was the highest (18.54 mm^{-2}) for the plants from the coarse sand desert and the lowest (6.67 mm^{-2} – 8.67 mm^{-2}) for the two populations from the Cholistan desert margin and saline waterlogged area. The largest stomatal area ($3523.25 \mu\text{m}^2$) was recorded in the plants from the roadside, while lowest ($1577.81 \mu\text{m}^2$) was recorded in the plants from saline waterlogged area (Table 3, Fig. 8).

3.4.4. Multivariate analysis

3.4.4.1. Principal component analysis (PCA). Principal component analysis (PCA) demonstrated the effects of soil physicochemical characteristics on the morpho-anatomical and physiological attributes of *S. vera* in different salt affected habitats (Fig. 9). A closer alignment of eigenvectors in the same direction indicated a significant association of the variable components with the discriminating effect of soil physicochemical properties across different saline habitats. The PCA biplot for these traits was highly influential, with the first two principal components (Dim 1 and Dim 2) explaining 57.6 % and 14.6 % of the variation, respectively, for a total cumulative contribution of 72.2 %.

Soil variables (ECe, Na^+ , Cl^-) were strongly associated and clustered on the positive side of Dim 1 with relatively high eigenvalues. These variables were correlated with growth traits (RL, SL, RFW, SFW, RDW, SDW, RWC, SWC, SUC, LA), photosynthetic pigments (Chl a, Chl b, T. Chl, Car), organic osmolytes (Pro, TAA, TSP), enzymatic antioxidants (CA, SOD, POD), tissue ionic contents (R.Na^+ , S.Na^+ , R.Cl^- , S.Cl^- , R.Ca^{2+} , S.Ca^{2+} , S.K^+), and leaf anatomical traits (LLT, LST, LPT, LXA, LPA) in both saline desert and waterlogged habitats. Stem anatomical traits (SVA, SMX and SPA) and soil variables including organic matter and PO excelled toward the positive side of Dim 2, with strong association and high positive eigen values in the dryland salinity habitat. The RMX, RPA, SST, SPCA, SPT and soil PO were predominantly concentrated on the positive side of Dim 1 in the Coarse sand desert. Soil Ca^{2+} and root anatomy (RCT, RCCA and StA) showed negative loadings of eigenvalues in the Thal-desert margin and saline dune desert. The pH, SP and anatomical traits (SCT, SCCA, SET, RtA and R.K) were plotted near the center, reflecting no significant contribution to variations in either the Cholistan desert margin or saline inundation (Fig. 9).

3.4.4.2. Correlation matrix and clustered heatmaps.

A correlation matrix

Table 3Anatomical traits of *Suaeda vera* populations collected from variously salt affected habitats.

Ecological Habitats	SD	SW	SI	CS	DS	TD	CD	DD	RD	F-ratio	P value
Root anatomy											
RtA (mm^2)	0.71 ± 0.01 ^e	0.89 ± 0.08 ^b	0.98 ± 0.09 ^a	0.84 ± 0.01 ^c	0.60 ± 0.05 ^f	0.85 ± 0.02 ^c	0.92 ± 0.02 ^{ab}	0.78 ± 0.05 ^d	0.65 ± 0.01 ^f	116.10	<0.001***
RCT (μm)	Dis-integrated	Dis-integrated	85.02 ± 1.28 ^e	231.44 ± 1.85 ^c	33.06 ± 1.93 ^f	330.63 ± 6.88 ^a	335.35 ± 21.34 ^a	170.04 ± 2.25 ^d	292.84 ± 1.02 ^b	301.57	<0.001***
RCCA (μm^2)	Dis-integrated	Dis-integrated	999.16 ± 7.43 ^f	2471.61 ± 7.04 ^d	683.63 ± 10.87 ^g	3733.71 ± 6.36 ^a	3681.12 ± 23.56 ^b	2261.26 ± 11.63 ^e	2787.14 ± 13.63 ^c	74.72	<0.001***
RMX (μm^2)	5889.8 ± 37.21 ^b	1209.5 ± 7.54 ^h	473.28 ± 1.34 ⁱ	5416.51 ± 33.76 ^c	6941.55 ± 38.79 ^a	1735.38 ± 5.98 ^f	1525.03 ± 117.67 ^g	2471.61 ± 14.50 ^d	2050.91 ± 18.71 ^e	62.67	<0.001***
RPA (μm^2)	6047.5 ± 41.85 ^a	2103.5 ± 15.36 ^h	2576.79 ± 13.79 ^g	5784.63 ± 41.64 ^b	4627.7 ± 28.05 ^c	1893.152 ± 10.57 ⁱ	3733.71 ± 23.63 ^d	2734.55 ± 21.64 ^f	3838.89 ± 20.47 ^e	8.29	<0.001***
RSrA (mm^2)	0.67 ± 0.87 ^b	0.87 ± 0.05 ^a	0.82 ± 0.06 ^a	0.6b ± 0.02 ^c	0.32 ± 0.01 ^e	0.23 ± 0.01 ^f	0.55 ± 0.02 ^c	0.45 ± 0.01 ^d	0.21 ± 0.01 ^f	493.96	<0.001***
RST (μm)	1048.58 ± 3.25 ^c	1232.79 ± 5.97 ^a	1199.72 ± 6.36 ^b	939.94 ± 7.64 ^d	722.67 ± 5.88 ^e	429.82 ± 5.54 ^g	949.39 ± 10.97 ^d	538.46 ± 7.58 ^f	595.14 ± 4.95 ^f	635.94	<0.001***
Stem anatomy											
STA (mm^2)	1.21 ± 0.10 ^b	1.07 ± 0.03 ^c	1.32 ± 0.10 ^a	0.98 ± 0.08 ^d	1.01 ± 0.11 ^{cd}	1.03 ± 0.06 ^{cd}	1.004 ± 0.05 ^d	0.86 ± 0.05 ^e	0.79 ± 0.06 ^f	153.34	<0.001***
SET (μm)	103.91 ± 3.09 ^b	51.95 ± 1.50 ^f	118.08 ± 1.38 ^a	51.95 ± 1.93 ^g	37.78 ± 0.85 ^h	75.57 ± 2.03 ^e	94.46 ± 2.54 ^c	89.74 ± 2.23 ^d	33.061 ± 1.02 ⁱ	71.78	<0.001***
SECA (μm^2)	2944.9 ± 13.36 ^b	1419.86 ± 2.78 ^e	3365.6 ± 14.79 ^a	1682.8 ± 7.67 ^d	841.4 ± 10.54 ^g	1367.27 ± 5.76 ^f	2944.91 ± 13.63 ^b	1945.74 ± 11.64 ^c	525.87 ± 4.25 ^h	27.72	<0.001***
SCT (μm)	155.87 ± 6.63 ^d	141.7 ± 4.49 ^e	406.2 ± 5.06 ^a	146.42 ± 3.08 ^e	99.19 ± 1.14 ^g	292.84 ± 2.87 ^b	297.57 ± 2.98 ^b	193.65 ± 3.95 ^c	108.63 ± 4.05 ^f	169.18	<0.001***
SCCA (μm^2)	1051.75 ± 9.571 ^h	1367.27 ± 8.75 ^f	10,307.16 ± 18.95 ^a	3155.25 ± 10.74 ^d	1104.33 ± 4.12 ^g	6836.38 ± 41.64 ^b	6520.86 ± 25.76 ^c	6783.79 ± 35.67 ^b	1472.45 ± 14.07 ^e	189.61	<0.001***
SVB (μm^2)	17,143.54 ± 29.51 ^d	17,511.66 ± 38.79 ^d	14,724.51 ± 28.83 ^f	43,069.21 ± 74.11 ^a	34,970.73 ± 57.24 ^b	14,093.46 ± 29.08 ^f	13,462.41 ± 74.11 ^g	15,460.74 ± 48.54 ^e	32,236.17 ± 41.90 ^c	40.49	<0.001***
SMX (μm^2)	736.22 ± 10.57 ^g	893.98 ± 8.89 ^f	1104.33 ± 7.70 ^d	3313.01 ± 10.54 ^a	2997.49 ± 15.25 ^b	1051.75 ± 8.75 ^e	368.11 ± 5.54 ^h	371.15 ± 2.95 ^h	2524.2 ± 7.71 ^c	59.89	<0.001***
SPA (μm^2)	3365.6 ± 18.97 ^f	3418.19 ± 11.75 ^f	2892.31 ± 15.59 ^g	6100.15 ± 25.87 ^a	5679.45 ± 11.94 ^b	4469.94 ± 18.23 ^e	2734.55 ± 10.95 ^g	4575.11 ± 14.75 ^d	4943.23 ± 12.70 ^c	18.19	<0.001***
SSB (μm)	89.74 ± 1.09 ^a	51.73 ± 2.01 ^g	70.85 ± 1.75 ^c	75.57 ± 1.19 ^b	66.12 ± 3.08 ^d	51.95 ± 1.01 ^g	47.23 ± 2.07 ^h	56.51 ± 2.25 ^f	61.17 ± 3.75 ^e	2.99	0.015**
SST (μm)	425.1 ± 4.53 ^a	410.93 ± 2.60 ^b	358.97 ± 3.78 ^c	103.91 ± 1.87 ^e	118.08 ± 2.14 ^d	113.36 ± 1.97 ^d	368.42 ± 3.25 ^c	118.09 ± 1.14 ^d	108.63 ± 1.37 ^e	442.57	<0.001***
SPT (μm)	987.17 ± 9.77 ^a	623.48 ± 4.89 ^b	429.82 ± 4.56 ^d	921.05 ± 10.54 ^a	680.16 ± 4.57 ^b	467.61 ± 3.81 ^d	193.65 ± 2.01 ^e	458.16 ± 3.21 ^d	519.56 ± 5.57 ^c	13.90	<0.001***
SPCA (μm^2)	3944.06 ± 20.47 ^d	6310.51 ± 17.54 ^a	3155.25 ± 7.56 ^g	4943.23 ± 4.43 ^b	4575.11 ± 5.12 ^c	3365.61 ± 7.45 ^f	2734.55 ± 4.65 ^h	3786.31 ± 10.89 ^e	3996.65 ± 11.56 ^d	11.07	<0.001***
Leaf anatomy											
LLT (μm)	788.79 ± 10.86 ^c	954.11 ± 9.29 ^a	850.2 ± 10.57 ^b	736.84 ± 11.92 ^d	708.5 ± 5.57 ^{de}	680.16 ± 12.54 ^e	642.37 ± 12.34 ^{ef}	552.63 ± 5.74 ^f	377.86 ± 4.12 ^g	367.04	<0.001***
LET (μm)	113.36 ± 3.95 ^a	118.08 ± 5.58 ^a	89.74 ± 2.97 ^b	89.74 ± 2.12 ^b	51.95 ± 1.75 ^e	75.57 ± 1.42 ^d	80.29 ± 1.21 ^c	80.29 ± 2.57 ^c	37.78 ± 1.02 ^f	7.65	<0.001***
LECA (μm^2)	5311.34 ± 38.76 ^b	5942.39 ± 21.45 ^a	5994.98 ± 47.54 ^a	4680.29 ± 20.97 ^c	4207.97 ± 11.51 ^f	4312.17 ± 19.87 ^e	4522.53 ± 28.02 ^d	3944.06 ± 24.75 ^g	2839.32 ± 12.48 ^h	4.76	0.01
LPT (μm)	122.81 ± 1.23 ^b	146.42 ± 1.87 ^a	108.63 ± 0.97 ^d	118.08 ± 2.10 ^c	75.57 ± 1.01 ^f	66.12 ± 0.87 ^g	89.74 ± 1.03 ^e	61.4 ± 2.1 ^g	51.95 ± 0.80 ^h	20.01	<0.001***
LST (μm)	486.51 ± 3.93 ^c	552.63 ± 10.04 ^a	519.56 ± 6.84 ^b	486.501 ± 3.96 ^c	429.82 ± 5.38 ^{cd}	401.48 ± 4.01 ^d	387.31 ± 3.66 ^e	297.57 ± 4.52 ^f	151.14 ± 2.19 ^g	136.61	<0.001***
LSCA (μm^2)	13,567.59 ± 96.92 ^b	12,358.07 ± 81.8 ^c	17,879.77 ± 67.15 ^a	11,201.1 ± 74.67 ^d	10,412.33 ± 61.54 ^e	9991.63 ± 66.01 ^f	9886.46 ± 56.54 ^f	4417.35 ± 51.20 ^g	4259.59 ± 47.22 ^h	6.60	<0.001***

(continued on next page)

Table 3 (continued)

Ecological Habitats	SD	SW	SI	CS	DS	TD	CD	DD	RD	F-ratio	P value
LTVB (μm^2)	27.94 \pm 0.47 ^a	22.42 \pm 0.84 ^b	24.97 \pm 0.75 ^{ab}	25.37 \pm 0.66 ^{ab}	17.94 \pm 0.22 ^c	21.14 \pm 1.07 ^b	18.31 \pm 1.22 ^c	17.2 \pm 0.98 ^c	10.17 \pm 0.05 ^d	5.25	0.002**
LXA (μm^2)	5153.58 \pm 41.64 ^a	2681.96 \pm 22.87 ^c	3418.19 \pm 28.97 ^b	3575.95 \pm 20.54 ^b	2103.51 \pm 18.44 ^d	2576.79 \pm 37.50 ^c	2261.26 \pm 24.51 ^d	1893.15 \pm 18.70 ^c	1156.92 \pm 9.58 ^f	8.70	<0.001***
LPA (μm^2)	4154.41 \pm 3361 ^a	2839.72 \pm 23.63 ^c	2629.37 \pm 21.45 ^d	3365.61 \pm 19.87 ^b	1945.74 \pm 6.99 ^g	2471.61 \pm 10.74 ^e	2103.51 \pm 11.66 ^f	1525.03 \pm 12.93 ^h	1262.11 \pm 7.04 ⁱ	465.62	<0.001***
Std (mm ²)	11.35 \pm 0.85 ^c	8.67 \pm 1.54 ^e	10.66 \pm 2.12 ^{cd}	18.54 \pm 1.88 ^a	9.66 \pm 1.85 ^d	6.67 \pm 0.88 ^f	9.23 \pm 2.25 ^d	14.11 \pm 1.87 ^b	11.45 \pm 2.21 ^c	50.57	<0.001***
StA (μm^2)	1893.21 \pm 15.02 ^f	1577.81 \pm 25.30 ^h	1682.15 \pm 19.99 ^g	473.79 \pm 18.59 ^j	2997.19 \pm 20.04 ^d	3418.12 \pm 18.87 ^b	2576.28 \pm 12.94 ^f	3313.01 \pm 15.67 ^c	3523.25 \pm 21.83 ^a	8.40	<0.001***

Means \pm SE ($n = 16$); Means sharing different letters indicate significant differences at $P \leq 0.05$ (LSD test), ** significance at $P \leq 0.01$, *** significance at $P \leq 0.001$.

Anatomical characteristics: Rta-root area, RCCA-root cortex thickness, RMX-root metaxylem vessel area, RPA-root phloem area, RST-root sclerenchyma thickness, STA-stem area, SET-stem epidermal thickness, SECA-stem cortical cell area, SCT-stem cortex thickness, SVA-stem vascular bundle area, SPA-stem phloem area, SSB-stem sclerenchyma thickness, SST-stem bundle thickness, LPT-leaf palisade thickness, LLT-leaf spongy thickness, LET-leaf lamina thickness, LXA-leaf pit cell area, LTVB-leaf spongy cell area, LPA-leaf xylem area, LSCA-leaf phloem area, StA-leaf stomatal density, and STA-stomatal area.

Ecological Habitats: SD: Saline desert; SW: Saline waterlogged area; SI: Saline inundations; CS: Coarse sand desert; DS: Dryland salinity; TD: Thal desert margin; CD: Cholistan desert margin; DD: Sand dune desert; RD: Roadside.

between the soil properties and morphological traits revealed significant positive correlations between soil the ECe, Na⁺, Cl⁻ and the RL, SL, LA, RFW, RDW, RWC, SFW, SDW, SWC and SUC. However, soil Ca²⁺, K⁺ and NO were strongly negatively correlated with all growth attributes (Fig. 10a). A clustered heatmap was generated between soil properties and morphological traits to evaluate their response across different habitats (Fig. 11a). The soil ECe, Na⁺, Cl⁻ and RL were strongly associated with each other and clustered in the saline desert habitat, while the soil ECe, Na⁺, Cl⁻ and RFW, RDW, RWC, SFW, SDW, SWC, SL, LA, SUC and RL in saline waterlogged area. However, the aforementioned variables were also correlated with the saline inundation habitat. At the roadside, all the growth attributes and the soil ECe, Na⁺, and Cl⁻ contents were negatively associated with each other (Fig. 11a).

The soil physicochemical properties strongly influence the physiological attributes, as shown in Fig. 10b. A significant positive relationship was found between ECe, Na⁺, Cl⁻ and CAT, SOD, Pro, Car, R, Na⁺, S, Na⁺, R, Cl⁻, S, Cl⁻ and photosynthetic pigments. Soil Ca²⁺ was negatively associated with POD, Pro, S, Na⁺, S, Cl⁻ and R, Ca²⁺ (Fig. 10b). The clustered heatmap of soil and physiological attributes revealed close associations and groupings of soil ECe, Na⁺, Cl⁻, pH, SP and CAT, Car, Pro, SOD, POD, Chl. a, Chl. b, R, Na⁺, S, Na⁺, R, Cl⁻, S, Cl⁻, R, Ca²⁺, S, Ca²⁺ in saline waterlogged area and saline desert habitats (Fig. 11b). All of the aforementioned attributes as well as R, K⁺ and S, K⁺ were positively associated with the saline inundation habitat. Strong negative relationships were recorded between soil NO, Ca, SP, and K⁺ and all growth attributes at the roadside and between soil pH and S, K⁺ in the coarse sand desert (Fig. 11b).

In terms of the relationships between soil and root anatomical attributes, soil ECe, Na⁺ and Cl⁻ were positively related to root RSRA and RST, whereas soil K⁺ and Ca²⁺ had a negative relationship with the aforementioned attributes and were positively associated with RCT and RCCA (Fig. 10c). In terms of the clustered heatmaps, the soil ECe, Na⁺, Cl⁻, SP and RTA, RST, and RSRA were strongly clustered in the saline waterlogged and saline inundation habitats (Fig. 12a). In the saline desert, soil ECe, Na⁺, and Cl⁻ positively clustered with RPA and RMX. The soil NO, SP, K⁺, and Ca²⁺ concentrations and RTA, RST, and RSRA concentrations at the roadside and the soil OM, ECe, Na⁺, Cl⁻ and RCT, RCCA in the cholistan desert margin and soil SP and RCT, and RCCA concentrations at the Thal-desert margin had strong negative associations. In terms of dryland salinity, a negative association was observed between soil pH and RMX (Fig. 12a).

The correlation matrix for soil and stem anatomical attributes and soil ECe, Na⁺, and Cl⁻ were positively associated with stem StA, SSB and SST; pH was positively associated with SET; and PO and OM were positively associated with SPA; and K⁺, NO and Ca²⁺ were negatively associated with Sta (Fig. 10d). In the case of the soil and stem anatomical attribute heatmaps, soil PO, OM and stem SPA, SPT, SVA, SMX, SST and SPCA showed positive clustering in both the coarse sand desert and dryland salinity. In a saline desert habitat, soil ECe, Na⁺, and Cl⁻ had strong positive relationships with SST and SPCA, and with SPT in a saline waterlogged area. Strong negative correlations were detected between soil NO, Cl⁻, K⁺, and SP and StA, SSB, SET and SECA at the roadside (Fig. 12b).

Strong positive correlations were found between soil ECe, Na⁺, Cl⁻ and leaf traits such as LPA, LXA, LTVB, LPT, LET, LLT, LST, LECA, and LSCA, while negative correlations were found between K⁺, and Ca²⁺ and all the aforementioned leaf traits (Fig. 10e). The clustered heatmap of soil and leaf anatomical attributes indicated strong positive clustering of soil ECe, Na⁺, and Cl⁻ with LPA, LXA, LTVB, LPT, LET, LLT, LST, LECA and LSCA in saline desert, saline waterlogged area and in saline inundation habitats. However, PO, SP, K⁺, and Ca²⁺ were strongly negatively clustered with the aforementioned leaf anatomical attributes at the roadside soil, in coarse sand desert soil pH with all leaf attributes except StA, and in sand dune desert soil pH, PO, OM, K⁺, and Ca²⁺ with LSCA, LPT, LPA, LST, and LLT (Fig. 12c).

SD-Saline desert: Reduced root area (R); cortical parenchymatous region (Co) disintegrated, heavily sclerified stellar region (St); with enlarged metaxylem vessels (Mx) arranged in two rings	SW-Saline waterlogged area: Root comprising enlarged, sclerified rings of vascular tissues (VT) containing numerous small metaxylem vessels (Mx); cortical region disintegrated (Co); intensively sclerified stellar region (St)	SI-Saline inundation: Enlarged root cross-sectional area (R); metaxylem vessel (Mx) small and numerous; cortical region (Co) reduced and partially distorted, intensively sclerified stellar region (St)
CS-Coarse sand desert: Root comprises well-developed cortical region (Co); rings of vascular tissues (VT) with extraordinary broad xylem vessels (Mx) and sclerified stellar region (St)	DS-Dryland salinity: Reduced root area (R) with thin and partially distorted cortical region (Co); enlarged metaxylem vessels (Mx) arranged in two rings, outer (beneath the cortex) have large than inner; sclerified stellar region (St)	TD-Thal desert margin: Root with thick cortical region (Co); stellar region (St) slightly sclerified comprising few small metaxylem vessels (Mx)
CD-Cholistan desert margin: Enlarged root cross sectional area with thick cortical region (Co); sclerified stellar region (St) comprising rings of compact vascular tissue (VT); metaxylem vessels (Mx); small and reduced	DD-Sand dune desert: Root area (R) slightly reduced, thin cortical region (Co) with enlarge cells (CC); few larger (outer ring) and numerous smaller (in stellar region) metaxylem vessels (Mx); minute development of sclerenchyma tissue in stellar region with compact ring of vascular tissue (VT)	RD-Roadside: Reduced root cross sectional area (R) with large cortical parenchymatous regions (Co); slightly sclerified stellar region (St) with numerous small metaxylem vessels

Fig. 5. Root transverse sections of *Suaeda vera* populations collected from various salt-affected habitats in Punjab province ($n = 16$, magnification= $40\times$ and $60\times$). The arrows with abbreviation labels in each habitat indicate prominent anatomical features.

SD-Saline desert: Enlarge stem area (S); thick intact epidermis (EP); highly developed sclerified bundles in cortical region (SB); sclerified stellar region (St); well develop pith (PI); narrow metaxylem vessels in ring form (Mx)	SW-Saline waterlogged area: Double layer epidermis with tightly packed epidermal cells (EC); extensive sclerification in stellar region (St); large pith cells (PC); metaxylem vessels (Mx) small and arranged in ring form around pith region	Enlarge stem area (S); thick intact epidermis (Ep); well-developed cortical region (Co); with sclerified bundles (SB); development of sclerenchyma in stelar region (St); small central vascular bundles (VB)
CS-Coarse sand desert: Stem with well-developed sclerified peripheral vascular bundles (VB) and metaxylem vessels (Mx); reduced cortical region with sclerified bundles (SB); larger pith area (PI)	DS-Dryland salinity: Stem with intact epidermis (Ep) and reduced cortical region (Co); large peripheral vascular bundles (VB) with metaxylem vessels (Mx); larger pith region (PI)	TD-Thal desert margin: Enlarge stem (S) with well-developed cortical region (Co) and small central vascular bundles (VB)
CD-Cholistan desert margin: Stem with sclerified epidermis (Ep) and cortical region (Co); sclerified stellar region (St) with highly reduced pith region (PI); vascular bundles (VB) and metaxylem vessels	DD-Sand dune desert: Stem area (S) reduced; intact double layer epidermis (Ep); cortical region with larger loosely arranged cells (CC)	RD-Roadside: Greatly reduced stem area (S); thin-walled epidermis (Ep); large peripheral tissues (VB) with broad metaxylem vessels, (Mx) and increased pith thickness (PI).

Fig. 6. Stem transverse sections of *Suaeda vera* populations collected from various salt-affected habitats of Punjab province ($n = 16$, magnification= 40 \times and 60 \times). The arrows with abbreviation labels in each habitat indicate prominent anatomical features.

3.5. Phytoremediation attributes

The root and shoot bioconcentration factor (BCF) for Na^+ and Cl^- varied considerably across the different saline habitats (Table 4). For the

root Na^+ and Cl^- bioconcentration factor, the highest concentrations (up to 0.068) were observed in populations collected from the CD, DD and RD habitats, whose salinity level ranged from 1.77 to 10.27 dS m $^{-1}$), while populations collected from the SD and SW habitats exhibited

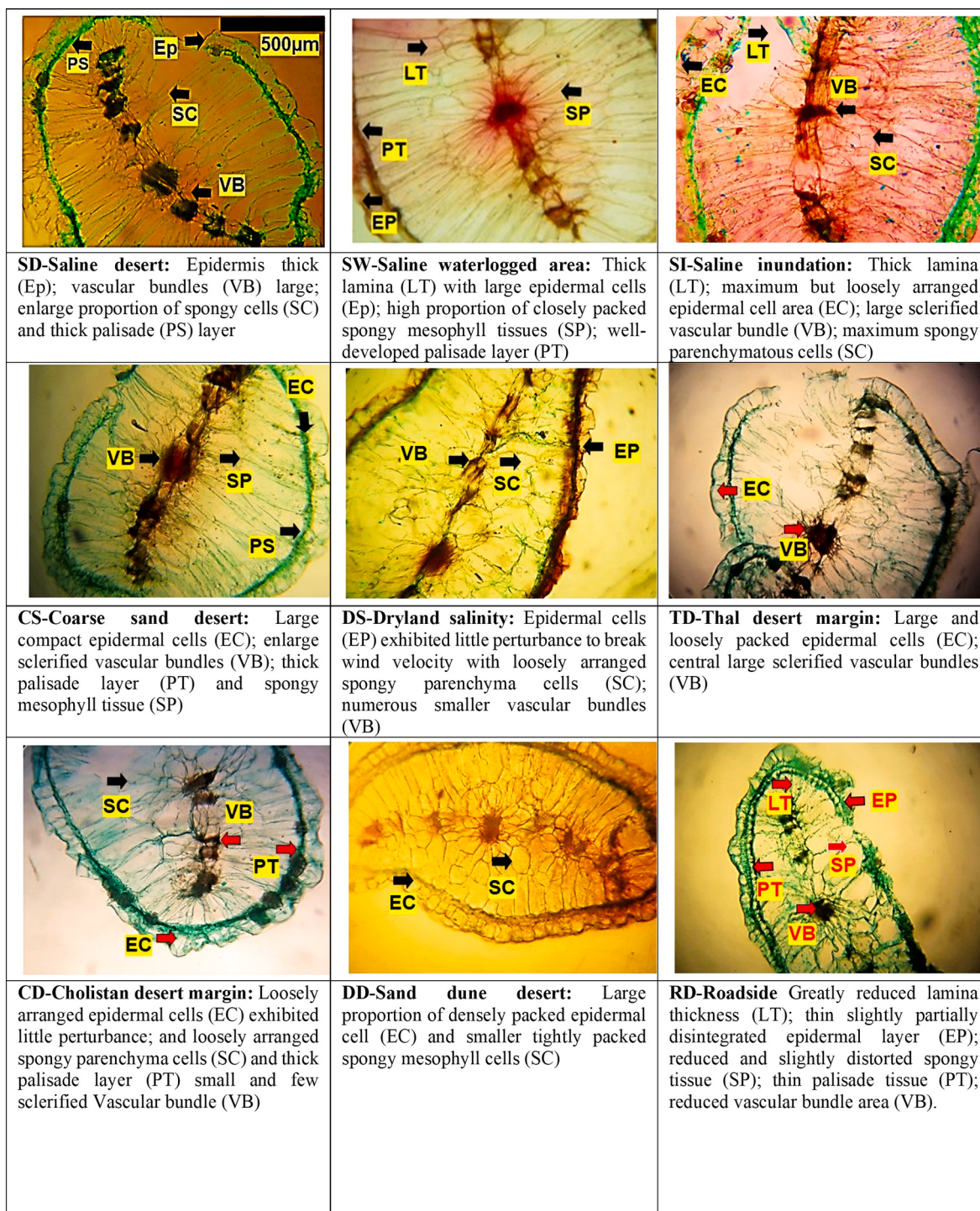


Fig. 7. Leaf transverse sections of *Suaeda vera* populations collected from various salt-affected habitats in Punjab province ($n = 16$, magnification= 40 \times and 60 \times). The arrows with abbreviation labels in each habitat indicate prominent anatomical features.

significantly lower BCF values. In contrast to the trend in the roots, the shoot bioconcentration factor for Na^+ and Cl^- increased progressively as the salinity of the habitat increased, indicating a direct correlation with salinity. The shoot Na^+ and Cl^- bioconcentration factors peaked (up to 1.69 and 1.123, respectively) in the highly saline SD, SW and SI populations, but significantly ($P \leq 0.05$) lower in the DD and RD populations with relatively low salinity (Table 4). A similar pattern emerged for the translocation factor (TF) for both Na^+ and Cl^- , with highly saline populations (SD, SW and SI) generally displaying elevated values, indicating a greater capacity to translocate salts to above ground parts.

In contrast, the lowest TF values were recorded in the least saline DD and RD populations. The maximum dilution factor (DF) values for root Na^+ and Cl^- (up to 21.5) were noted in the TD and CD populations, while those for shoot Na^+ and Cl^- were noted in the SW and SI populations (Table 4).

4. Discussion

Halophytes act as indicator species, providing valuable insights into the physicochemical composition of soil as well as the intensity and type

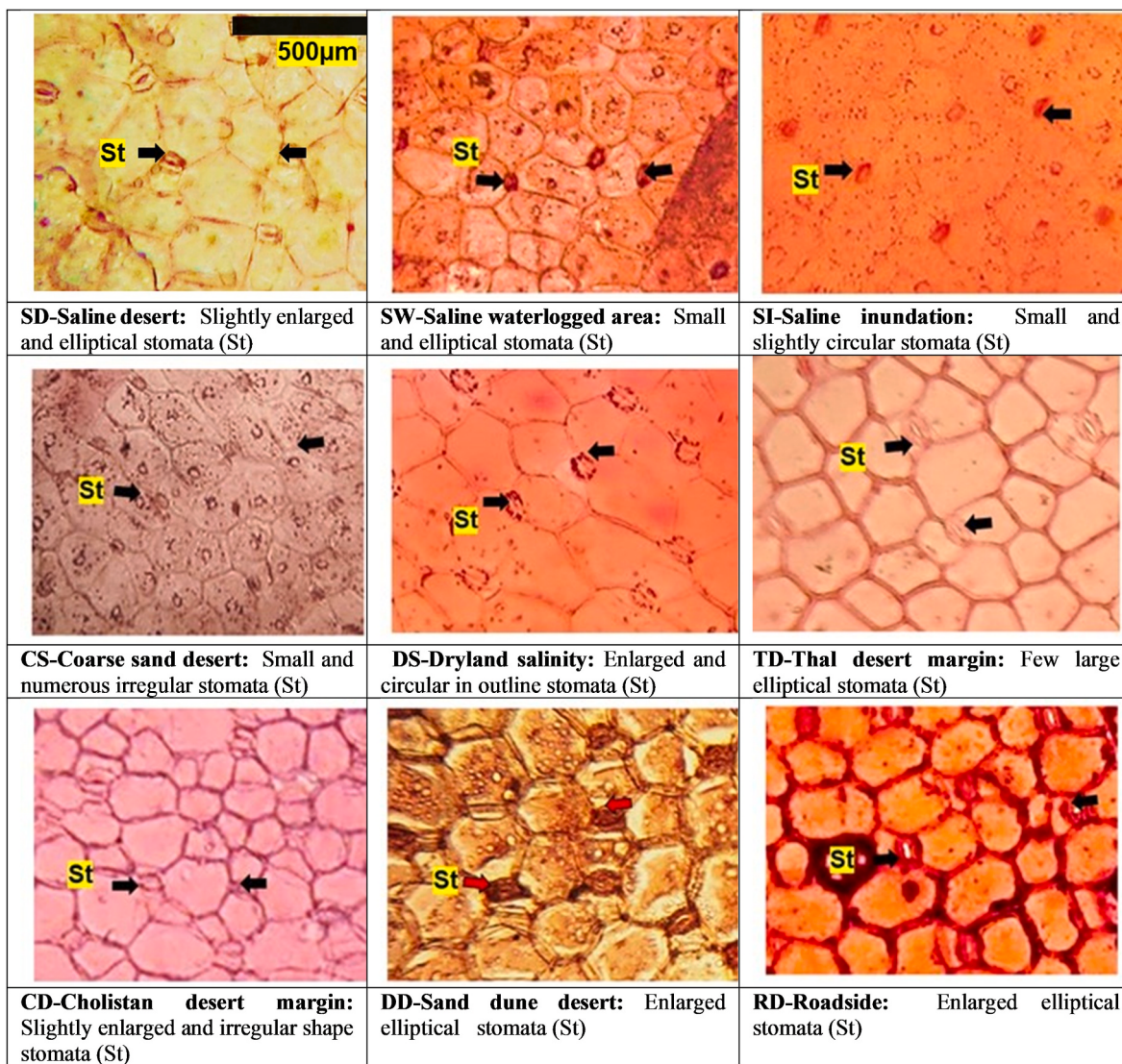


Fig. 8. Leaf epidermal attributes of *Suaeda vera* populations collected from various salt-affected habitats in Punjab province ($n = 16$, magnification= 40 \times and 60 \times). The arrows with abbreviation labels in each habitat indicate prominent anatomical features.

of salinity prevalent in natural saline habitats. Their presence and health reflect the specific characteristics of the soil, offering crucial information about the nature and composition of the saline environment (Asghar et al., 2023). Additionally, halophytes are beneficial in marginal lands, serving as forage crops and sources of bioenergy, while also demonstrating phytoremediation capabilities for soil improvement (Mujeeb et al., 2023; Abid et al., 2025). The success of plants in specific environments relies on comprehensive adjustments at the whole-plant level. *Suaeda vera* has a range of structural and functional adaptative mechanisms that enable it to endure effectively diverse environmental challenges (Fig. 13; Table 3).

In this study, we evaluated nine naturally occurring populations of *Suaeda vera* from a diverse range of saline habitats with salinity levels ranging from ECe 1.77 to 39.75 dS m⁻¹. The sampling of sixteen plants per population allowed us to capture significant morphological and physio-anatomical traits essential for salt tolerance and phytoremediation potential. While this sampling strategy effectively represents the key adaptive responses of *S. vera* populations across distinct saline environments including saline deserts, waterlogged areas, and inundated sites, we acknowledge that it may not fully encompass the entire genetic and phenotypic variability present across the species' full geographic distribution. Furthermore, our study focused primarily on

salinity gradients and did not incorporate other environmental factors such as microclimate, which could also influence trait expression. Additionally, while we assessed physiological mechanisms including ion accumulation, osmolyte content, and antioxidative enzyme activity, these represent snapshots in time; thus, temporal variations and underlying molecular regulatory processes remain to be explored. Despite these simplifications and data gaps, the consistent patterns of anatomical and biochemical adaptations observed across multiple populations provide robust evidence of the ecological resilience and phytoremediation capacity of *S. vera*. Future research expanding sampling breadth, integrating environmental covariates, and applying molecular approaches will be critical to fully understand the mechanisms driving adaptation and to optimize the use of this species in sustainable management of saline soils. Overall, our study offers a valuable and justified contribution toward characterizing the salt tolerance traits of *S. vera* and supports its practical application in phytoremediation programs.

4.1. Growth response of salt tolerant plants in saline habitats

Salt-tolerant plants exhibit enhanced growth under saline conditions through improved morphological traits (Yuan et al., 2019). Among the

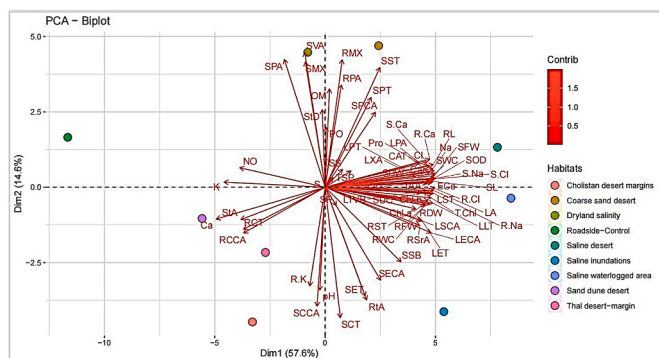


Fig. 9. Principal component analysis (PCA) showing the influence of contributing factors (soil) on morphological, physiological and anatomical attributes of *Suaeda vera* populations from diverse habitats of Punjab province. Dim1 (57.6 %) and Dim2 (14.6 %) explain a cumulative 72.2 % of total variance. Populations from different habitats are represented by color coded dots. Dark red vectors: indicates high contribution of traits to the principal components. **Soil:** pH- soil pH, ECe-soil electrical conductivity, OM-soil organic matter, SP- soil saturation percentage, Na-soil Na⁺, K-soil K⁺, Ca-soil Ca²⁺, Cl-soil Cl, NO-soil NO₃, PO-soil PO₄³⁻; **Plant morphology:** LA-leaf area, RL-root length, SL-shoot length, RFW- root fresh weight, RDW- root dry weight, RWC- root water content, SFW-shoot fresh weight, SDW-shoot dry weight, SWC-shoot water content, Suc-succulence; **Plant physiology:** R. Ca-root Ca²⁺, R. Cl-root Cl⁻, R. K- root K⁺, R. Na-root Na⁺, S. Ca-shoot Ca²⁺, S. Cl-shoot Cl⁻, S. K- shoot K⁺, S. Na-shoot Na⁺, TSP-total soluble proteins, TAA-total free amino acids, TSS-total soluble sugars, Pro-proline, CAT-catalase, POD-peroxidase, SOD-superoxide dismutase; **Anatomy:** RMX-root metaxylem cell area, RSaR-a root stelar region area; RTa-root area, RCT-root cortical thickness, RCCA-root cortical cell area, RST-root sclerenchyma thickness, RPA-root phloem area; **Stem anatomy:** STA-stem area, SET-stem epidermis thickness, SECA-stem epidermal cell area; SCT-stem cortical thickness, SCCA-stem cortical cell area, SSB- stem sclerified bundle thickness, SPT-stem pith thickness, SPCA-stem pith cell area, SMX-stem metaxylem area, SST-stem sclerenchyma tissue thickness, SPA-stem phloem area, SVA-stem vascular bundle area; **Leaf anatomy:** LLT-leaf lamina thickness, LET-leaf epidermal thickness, LECA-leaf epidermal cell area, LSCA-leaf spongy cell area, LLST-leaf spongy tissue thickness, LPT-leaf palisade thickness, LTVB- leaf total vascular bundle area, LXa-leaf xylem area, LPA-leaf phloem area, StA-stomatal density, StD-stomatal area.

S. vera populations, those in saline waterlogged areas (SW) display maximum growth attributes, indicating higher salt tolerance compared than other populations did (Fig. 2). This aligns with findings in *Sesuvium portulacastrum* by Muchate et al. (2016), who reported increased biomass production under high salinity. Similar results were reported by Boestfleisch and Papenbrock (2017) and Atzori et al. (2017) in halophytes, where increased biomass indicates elevated salt tolerance. The dominance of halophytes in saline habitats is attributed to their need for optimal growth (Rozema and Schat, 2013). The maximum root and shoot biomass production in the two highly saline populations (SW, SI) revealed their highest tolerance and structural stability despite stress. The observed growth stimulation by salt (ECe, 26.43 to 39.75 dS m⁻¹) was linked to increased shoot water content, recorded at its maximum in these tolerant populations, as documented by Khan and Weber (2006). This compensatory mechanism supports earlier findings, linking increased water content and sodium ions accumulation with improved succulence and resilience to extreme salinity (Ogburn and Edwards, 2010; Eisa et al., 2017). In contrast, populations from habitats with low salinity experienced significantly reduced growth (Fig. 2). The differential response is associated with the soil physicochemical characteristics of their respective habitats, indicating that halophytes necessitate a substantial amount of Na⁺ for their optimal growth (Song and Wang, 2015). The formation of longer roots in the saline desert population (SD) of a plant species represents a crucial ecological adaptive strategy. Salinity often induces physiological drought, as noted by Thorup-Kristensen et al. (2020). In response, an increase in root length may

serve as an advantageous trait by assisting in water uptake from deeper soil layers (Shaar-Moshe et al., 2017).

4.2. Physiological responses modulate osmotic regulation and salinity tolerance

The accumulation of inorganic ions particularly Na⁺ and Cl⁻, is a key strategy in many halophytes (Mahmuda et al., 2022). In highly saline (SD) environments, plants exhibit increased Na⁺ concentrations in their tissues, serving as an effective indicator of salinity tolerance through stimulated Na⁺ uptake (Maathuis et al., 2014). Elevated Na⁺ levels in the soil restrict K⁺ ions uptake due to competitive ion dynamics, particularly under hypersaline conditions (Khan et al., 2015). Concurrently, calcium (Ca²⁺) accumulation parallels elevated Na⁺ and chloride (Cl⁻) levels, as reported in other halophytic species (Khan et al., 2005; Joshi et al., 2022). Ionic selectivity (K^{+/Na⁺} and Ca^{2+/Na⁺}) increased under moderate salinity but decreased at extreme concentrations. Ca²⁺ plays a crucial role in maintaining cellular membrane integrity, regulating the K^{+/Na⁺} balance (Mahmood et al., 2009), and ultimately counteracting the adverse effects of Na⁺ and Cl⁻ (Kader and Lindberg, 2005). The influx of Ca²⁺ is actively engaged in reactive oxygen species (ROS) signaling, contributing to increased salt tolerance in plants (Flowers and Colmer, 2008; Mahmuda et al., 2022). In *S. vera*, the concentrations of Na⁺ and Cl⁻ ions increased in both the roots and the shoots (Fig. 3). Salinity-induced challenge elevate Na⁺ and Cl⁻ levels, which serve as economical osmotica in roots and shoots to reduce the osmotic potential (Isayenkov and Maathuis, 2019). The decrease in the levels of chlorophyll a (Chl a), chlorophyll b (Chl b), and carotenoids due to salinity have been documented in numerous halophytes (Haque et al., 2021; Joshi et al., 2023). This finding is consistent with the findings in the SD population of *S. vera*. Notably, SW population displayed a substantially greater Chl a, Chl b, and carotenoid concentrations (Fig. 3). This augmentation in the concentration of pigments seems to be closely linked to the photosynthetic efficacy of the studied populations when they are exposed to stressful circumstances (Maimaitiyiming et al., 2017).

Halophytes accumulate substantial quantities of low molecular weight organic osmolytes to mitigate oxidative stress via reactive oxygen species (ROS) quenching, stabilize proteins, maintain membrane integrity, and regulate osmotic balance, collectively increasing ionic stress tolerance under saline conditions (Surówka and Hura, 2020). In *S. vera* populations, there is a notable accumulation of organic osmolytes at high concentrations (Fig. 4). The marked tolerance of SD population is clearly associated with the maximal accumulation of total free amino acids and proline, thereby indicating superior osmotic adjustment and ionic homeostasis (Pan et al., 2016). Furthermore, the significant accumulation of organic solutes (total soluble sugars and proteins) within the dryland salinity (SD) population demonstrated their ability to withstand saline environments by increasing cell turgor and water levels. Additionally, the functionality of the trans-membrane proteins responsible for ion flux was enhanced, which collectively increased their potential for tolerating high salt concentrations (Kaleem et al., 2022). The adaptation of xero-halophytes to stress conditions, particularly high salinity, involves complex physiological and biochemical mechanisms. Antioxidants play a pivotal role in these adaptive responses by helping mitigate oxidative stress, a common consequence of environmental challenges. Oxidative stress occurs when there is an imbalance between the production of reactive oxygen species (ROS) and the plant's ability to detoxify them (Certain et al., 2021). The increased accumulation of antioxidant enzymes, such as superoxide dismutase (SOD), catalase (CAT), and peroxidase (POD), in xero-halophyte populations inhabiting heavily saline areas (SD and SW) highlights a robust defensive strategy against oxidative stress (Fig. 4). This adaptation is crucial for their survival in saline environments, demonstrating the ability of plants to counteract reactive oxygen species and alleviate the detrimental effects of salinity-induced stress (Ben Hamed et al., 2016a,b; Mahmuda et al.,

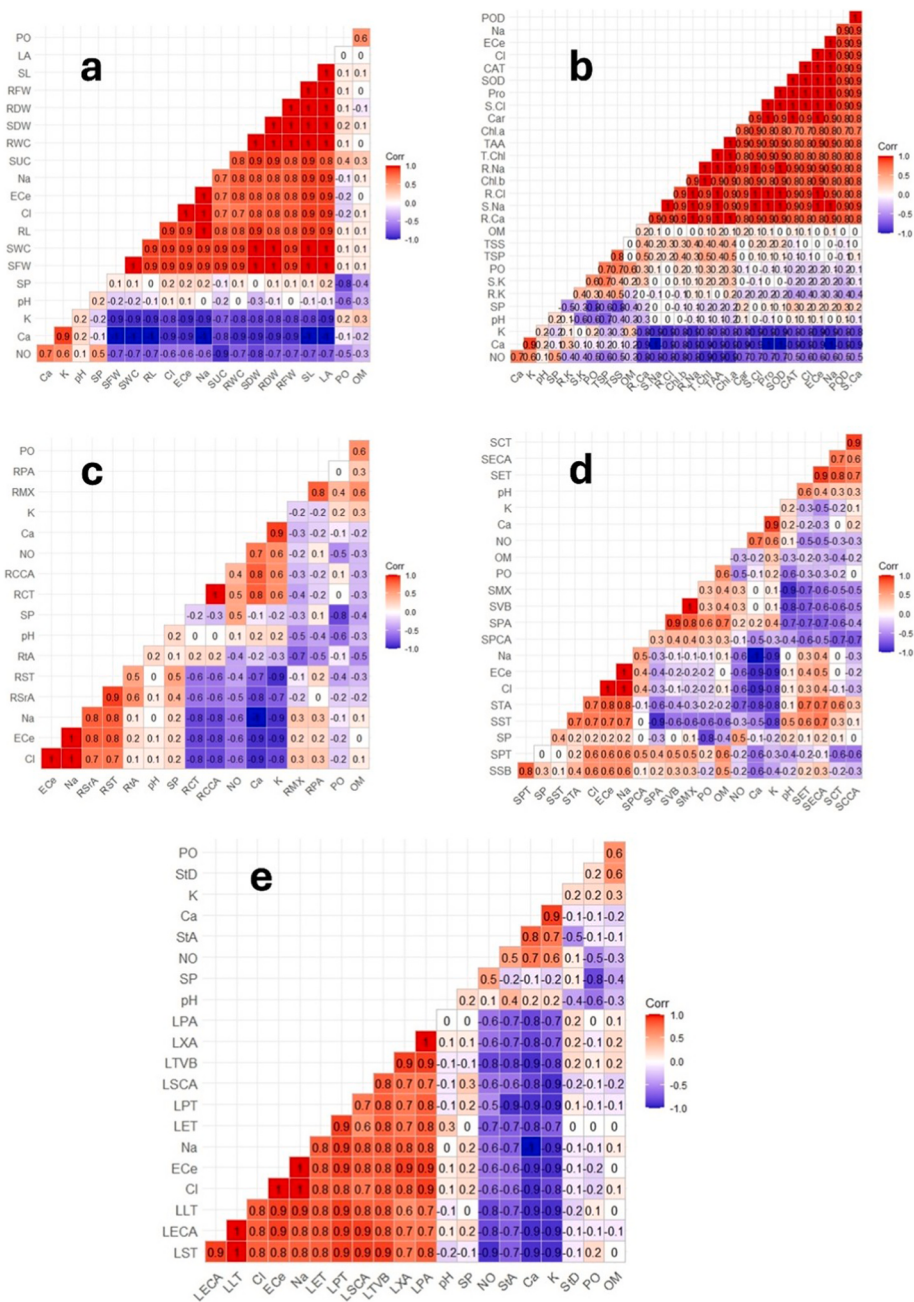


Fig. 10. Pearson's correlation matrix the relationships of soil physiochemical properties with (a) morphological, (b) physiological attributes, (c) root anatomy, (d) stem anatomy, and (e) leaf anatomy of *Suaeda vera* populations collected from various salt-affected habitats. Color gradient: Dark blue (close to -1.0): indicates a strong negative correlation; Light blue/white (near 0): indicates very weak or no correlation; Dark red (up to +1.0): indicates very strong positive correlation. **Soil:** pH-soil pH, EC_e-soil electrical conductivity, OM-soil organic matter, SP-soil saturation percentage, Na-soil Na⁺, K-soil K⁺, Ca-soil Ca²⁺, Cl-soil Cl, NO-soil NO₃, PO-soil PO₄³⁻; **Plant morphology:** LA-leaf area, RL-root length, SL-shoot length, RFW- root fresh weight, RDW- root dry weight, RWC- root water content, SFW-shoot fresh weight, SDW-shoot dry weight, SWC-shoot water content, Suc-succulence; **Plant physiology:** R, Ca-root Ca²⁺, R, Cl-root Cl⁻, R, K- root K⁺, R, Na-root Na⁺, S, Ca-shoot Ca²⁺, S, Cl-shoot Cl⁻, S, K- shoot K⁺, S, Na-shoot Na⁺, TSP-total soluble proteins, TAA-total free amino acids, TSS-total soluble sugars, Pro-Proline, CAT-catalase, POD-peroxidase, SOD-Superoxide dismutase; **Anatomy:** RMX-root metaxylem cell area, RSRA-root stelar region area, RTA-root area, RCT-root cortical thickness, RCCA-root cortical cell area, RST-root sclerenchyma thickness, RPA-root phloem area; **Stem anatomy:** STA-stem area, SET-stem epidermis thickness, SECA-stem epidermal cell area, SCT-stem cortical thickness, SCCA-stem cortical cell area, SSB- stem sclerified bundle thickness, SPT-stem pith thickness, SPCA-stem pith cell area, SMX-stem metaxylem area, SST-stem sclerenchyma tissue thickness, SPA-stem phloem area, SVA-stem vascular bundle area; **Leaf anatomy:** LLT-leaf lamina thickness, LET-leaf epidermal thickness, LECA-leaf epidermal cell area, LSCA-leaf spongy cell area, LLST-leaf spongy tissue thickness, LPT-leaf palisade thickness, LTVB- leaf total vascular bundle area, LXa-leaf xylem area, LPA-leaf phloem area, StD-stomatal density, StA-stomatal area.

2022).

4.3. Anatomical responses to salinity stress

Compared with morphological and physiological characteristics,

anatomical characteristics are more susceptible to environmental challenges (Mansoor et al., 2019). Plants originating from highly saline areas displayed a high degree of plasticity in terms of their root anatomical characteristics, indicating a key adaptive strategy to successfully thrive in saline extremes (Table 3, Fig. 5). The Root area was not strongly

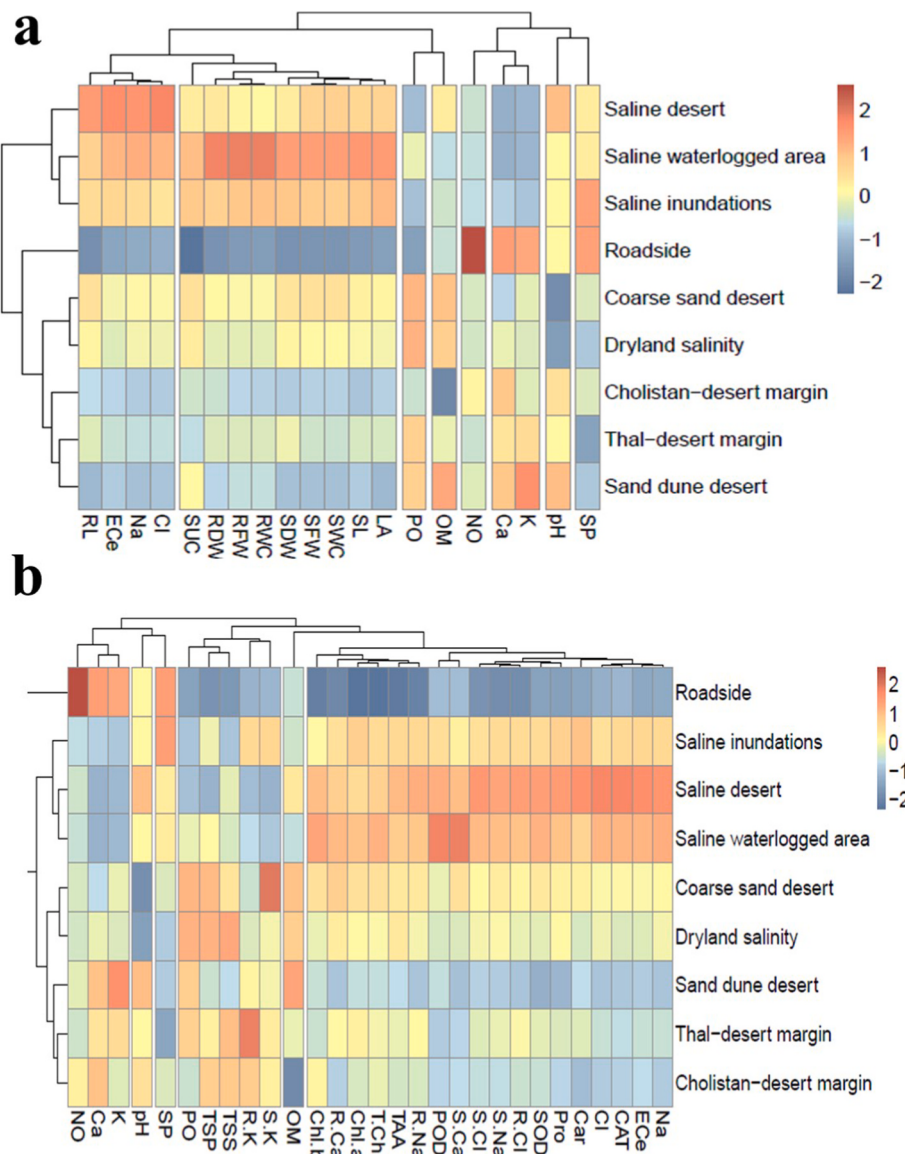
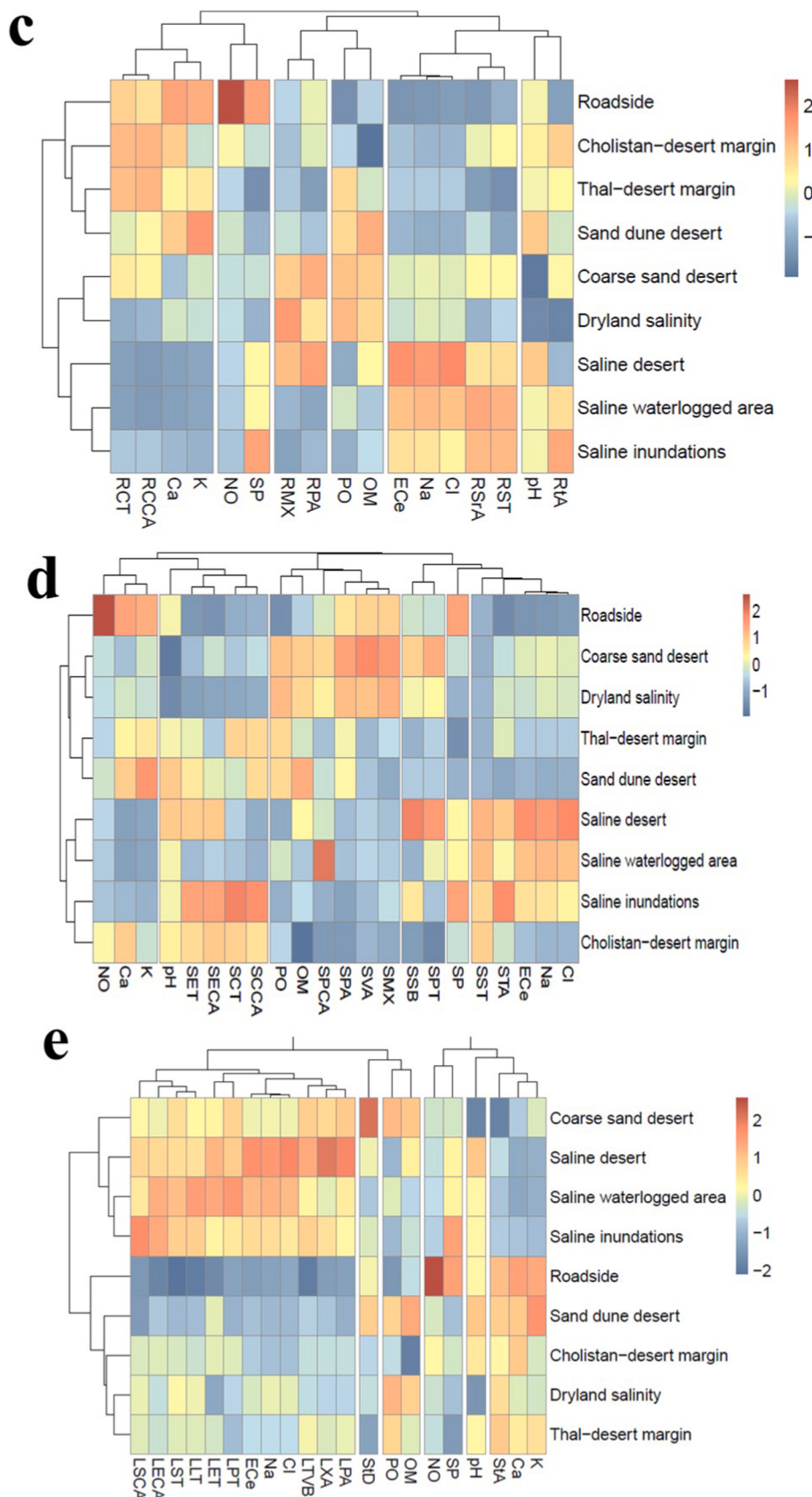


Fig. 11. Clustered heatmaps analysis representing the relationships between soil and morpho-physiological attributes of *Suaeda vera* populations collected from variously salt-affected habitats of Punjab province. Populations from distinct saline habitats are represented on the y-axis. Color gradient dark orange = high (+2), blue = low (-2) shows variables contribution and clustering shows traits and habitats similarity (a) Soil with morphological attributes (b) Soil with physiological attributes. **Soil:** pH-soil pH, ECe-soil electrical conductivity, OM-soil organic matter, SP-soil saturation percentage, Na-soil Na⁺, K-soil K⁺, Ca-soil Ca²⁺, Cl-soil Cl, NO-soil NO₃, PO-soil PO₄³⁻; **Plant morphology:** LA-leaf area, RL-root length, SL-shoot length, RFW- root fresh weight, RDW- root dry weight, RWC- root water content, SFW-shoot fresh weight, SDW-shoot dry weight, SWC-shoot water content, Suc-succulence; **Plant physiology:** R. Ca-root Ca²⁺, R. Cl-root Cl⁻, R. K- root K⁺, R. Na-root Na⁺, S. Ca-shoot Ca²⁺, S. Cl-shoot Cl⁻, S. K- shoot K⁺, S. Na-shoot Na⁺, TSP-total soluble proteins, TAA-total free amino acids, TSS-total soluble sugars, Pro-Proline, CAT-catalase, POD-peroxidase, SOD-Superoxide dismutase.

affected by soil salinity and was notably larger in the saline inundation habitat (SI). This finding suggests that increased root area is a strategic response to osmotic stress, improving the plant's ability to store and conduct water and nutrients, especially in highly saline environments (Kaleem and Hameed, 2021; Naz et al., 2024). This increase is attributed to a notable enhancement in sclerification within the root zone which is more prominent in the SW and SI populations. Intense sclerification in the stelar region of a root not only resists root collapse but also offers mechanical strength of the root, prevent water loss and is a defining feature of salt tolerance (Fatima et al., 2021; Ameer et al., 2023). Salt stress resulted in reduced or disintegrated root cortex region which were observed in three (SD, SW and SI) populations, which may reflect an adaptive trade-off to allocate nutrients from the soil-root interface to the roots and shoots (Zulfiqar et al., 2020). This finding is consistent with previous findings, suggesting that a reduced or disintegrated cortex

redirects resources toward more critical survival functions, potentially due to reduced metabolic activity in response to physiological drought (Iqbal et al., 2022; Asghar et al., 2023; Bibi et al., 2024). On the other hand, cortical thickness and cell area were significantly increased in Thal desert population (TD). The metaxylem area was highest in the populations thriving in the dryland saline region (DS) and saline desert (SD), where metaxylem vessels are arranged in two rings. The outer ring, positioned beneath the cortex, is larger than the inner ring and is characterized by a sclerified stelar region. The presence of larger metaxylem vessels enforces lower resistance to water and nutrient conduction under salt stress (Iqbal et al., 2023a, 2023b; Basharat et al., 2024).

The stem cross-sectional area increased in the population inhabiting the saline inundation (SI). The change in cross-sectional area in desert species proves to be more advantageous as it provides resistance against



(caption on next page)

Fig. 12. Clustered heatmaps analysis representing the relationship between soil and anatomical attributes of *Suaeda vera* populations collected from variously salt-affected habitats of Punjab province (c) Soil with root anatomy (d) Soil with stem anatomy (e) Soil with leaf anatomy. **Soil:** pH- soil pH, EC_e-soil electrical conductivity, OM-soil organic matter, SP- soil saturation percentage, Na-soil Na⁺, K-soil K⁺, Ca-soil Ca²⁺, Cl-soil Cl, NO-soil NO₃, PO-soil PO₄³⁻; **Anatomy:** RMX-root metaxylem cell area, RS_RA-root stellar region area, RT_A-root area, RCT-root cortical thickness, RCCA-root cortical cell area, RST-root sclerenchyma thickness, RPA-root phloem area; **Stem anatomy:** STA-stem area, SET-stem epidermis thickness, SECA-stem epidermal cell area, SCT-stem cortical thickness, SCCA-stem cortical cell area, SSB-stem sclerified bundle thickness, SPT-stem pith thickness, SPCA-stem pith cell area, SMX-stem metaxylem area, SST-stem sclerenchyma tissue thickness, SPA-stem phloem area, SVA-stem vascular bundle area; **Leaf anatomy:** LLT-leaf lamina thickness, LET-leaf epidermal thickness, LECA-leaf epidermal cell area, LSCA-leaf spongy cell area, LLST-leaf spongy tissue thickness, LPT-leaf palisade thickness, LTVB-leaf total vascular bundle area, LX_A-leaf xylem area, LPA-leaf phloem area, StD-stomatal density, StA-stomatal area.

Table 4

Na⁺ and Cl⁻ phytoremediation potential of *Suaeda vera* populations collected from variously salt affected habitats. (n = 16).

Ecological Habitats	Root BCF		Shoot BCF		TF		Root DF		Shoot DF	
	Na ⁺	Cl ⁻	Na ⁺	Cl ⁻	Na ⁺	Cl ⁻	Na ⁺	Cl ⁻	Na ⁺	Cl ⁻
SD	0.023 ± 0.004 ^h	0.021 ± 0.00 ⁱ	1.169 ± 0.17 ^a	1.123 ± 0.08 ^a	51.6 ± 2.67 ^a	56.371 ± 3.68 ^a	9.995 ± 1.89 ^g	8.731 ± 1.45 ^f	599.812 ± 18.94 ^d	617.616 ± 21.25 ^c
SW	0.024 ± 0.001 ^h	0.024 ± 0.002 ^h	1.133 ± 0.19 ^{ab}	1.120 ± 1.01 ^{ab}	47.522 ± 2.34 ^b	48.651 ± 2.15 ^b	16.249 ± 1.03 ^d	15.675 ± 1.36 ^d	910.744 ± 31.24 ^a	900.273 ± 35.66 ^a
SI	0.029 ± 0.002 ^g	0.029 ± 0.00 ^g	1.083 ± 0.15 ^{ab}	1.118 ± 1.11 ^b	36.524 ± 1.89 ^c	36.361 ± 2.45 ^c	15.021 ± 1.07 ^{de}	15.160 ± 1.03 ^d	736.212 ± 29.25 ^b	739.721 ± 23.66 ^b
CS	0.035 ± 0.001 ^e	0.034 ± 0.004 ^e	1.079 ± 0.11 ^b	1.105 ± 0.99 ^c	30.142 ± 1.58 ^d	31.870 ± 2.31 ^e	14.851 ± 1.32 ^e	14.380 ± 2.10 ^d	616.103 ± 14.56 ^c	631.595 ± 21.61 ^d
DS	0.033 ± 0.002 ^f	0.031 ± 0.002 ^f	1.060 ± 0.10 ^b	1.104 ± 1.21 ^c	31.487 ± 2.16 ^d	34.771 ± 1.25 ^d	12.075 ± 1.19 ^f	11.601 ± 0.99 ^e	559.901 ± 17.85 ^e	582.798 ± 23.89 ^e
TD	0.055 ± 0.003 ^d	0.054 ± 0.004 ^d	0.947 ± 0.09 ^c	0.979 ± 0.77 ^d	16.908 ± 1.09 ^e	17.826 ± 1.09 ^f	19.203 ± 2.23 ^b	18.953 ± 2.14 ^b	433.420 ± 12.30 ^f	450.658 ± 15.65 ^f
CD	0.068 ± 0.002 ^a	0.068 ± 0.005 ^b	0.932 ± 0.08 ^d	0.928 ± 0.89 ^e	13.691 ± 1.23 ^f	13.456 ± 1.22 ^g	21.577 ± 2.10 ^a	21.849 ± 2.74 ^a	282.926 ± 10.21 ^g	281.703 ± 18.23 ^g
DD	0.0613 ± 0.004 ^c	0.064 ± 0.004 ^c	0.851 ± 0.13 ^e	0.764 ± 0.14 ^f	13.435 ± 1.03 ^f	11.888 ± 1.22 ^h	17.074 ± 1.07 ^c	17.938 ± 2.39 ^c	229.896 ± 20.30 ^h	204.021 ± 14.39 ^h
RD	0.066 ± 0.004 ^b	0.088 ± 0.006 ^a	0.390 ± 0.19 ^f	0.468 ± 1.19 ^g	12.593 ± 2.15 ^g	5.309 ± 2.10 ⁱ	7.646 ± 1.09 ^h	10.118 ± 1.84 ^{ef}	115.751 ± 14.11 ⁱ	201.522 ± 11.97 ^h
F-ratio	701.95	1129.96	58.28	40.99	374.58	654.30	143.69	21.00	26,852	26,472.80
P value	<0.001***	<0.001***	<0.001***	<0.001***	<0.001***	<0.001***	<0.001***	<0.001***	<0.001***	<0.001***

Means ± SE (n = 16); Means sharing different letters indicate significant differences at P ≤ 0.05 (LSD test), ** significance at P ≤ 0.01, *** significance at P ≤ 0.001.

Legends: BCF: bioconcentration factor, TF: translocation factor, DF: dilution factor.

Ecological Habitats: SD: Saline desert; SW: Saline waterlogged area; SI: Saline inundations; CS: Coarse sand desert; DS: Dryland salinity; TD: Thal desert margin. CD: Cholistan desert margin; DD: Sand dune desert; RD: Roadside.

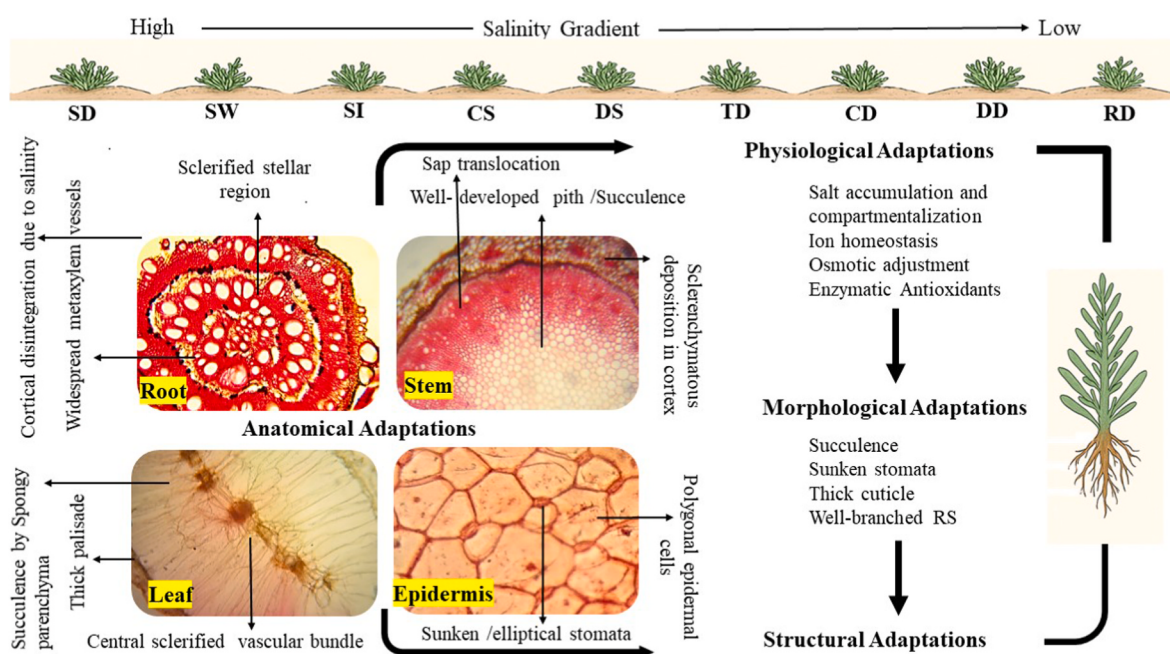


Fig. 13. Overall response of *Suaeda vera* populations to different salt-affected habitats. **Ecological Habitats:** SD: Saline desert; SW: Saline waterlogged area; SI: Saline inundations; CS: Coarse sand desert; DS: Dryland salinity; TD: Thal desert margin; CD: Cholistan desert margin; DD: Sand dune desert; RD: Roadside.

abiotic stresses. The enhancement in stem cross-sectional area, accompanied by storage parenchyma such as the cortex and pith, contributes to an increase in water storage capacity within the stem (Iqbal et al., 2021). Additionally, the population also displayed a significant enhancement in both the area and thickness of the epidermal cells when exposed to high salinity (Table 3, Fig. 6). This indicates a preferable strategy to regulate water loss in arid environments (Iqbal et al., 2021; Ameer et al., 2023). The anatomical characteristics of the stems, such as the area of vascular bundles, metaxylem and phloem, increased in populations of *S. vera* that managed to survive in the arid Cholistan desert (CD). This increase in the vascular region, as well as the diameter of the vessels and the area of phloem, undoubtedly plays a crucial role in facilitating the conduction of water, minerals, and photo-assimilates, especially under unfavorable circumstances (Kaleem and Hameed, 2021). In plants that thrive in a saline desert environment (SD), a general increase in the pith area and thickness is commonly observed (Table 3, Fig. 6). This phenomenon enhances succulence and is critically important for the survival of desert-dwelling species (Parida et al., 2016). Furthermore, the reinforcement of sclerenchyma bundles in all populations of *S. vera* under heavily saline conditions is highly important for providing mechanical strength during periods of salt stress and osmotic stress (Asghar et al., 2023).

4.4. Leaf succulence and ion homeostasis

The leaf internal architecture of *S. vera* displayed notable variations across different saline habitats, offering key insights into its environmental adaptability (Table 3, Fig. 7). The succulence of the leaves, particularly the thickness of the midrib and lamina, was found to increase in populations inhabiting saline waterlogged and inundation environments (SW and SI). The increased succulence was directly attributed to greater water storage spongy parenchymatous tissues, which may be due to larger leaf vacuoles that help sequester Na^+ away from the central metabolic processes of the cell (Chakraborty et al., 2018). Larger vacuoles facilitate the storage of ions and osmolytes, contributing to ion homeostasis in plant to cope with rapid increases in salt extremes (Loconsole et al., 2019; Asghar et al., 2023). In SW populations, increased succulence occurred in conjunction with shoot water content, palisade thickness and growth stimulation, suggesting its role in salinity tolerance (Table 3, Fig. 7). In addition to these changes, the population also exhibited an increase in the number and thickness of epidermal cells. Research indicates that plants that are tolerant to high salt levels often develop a thickened epidermis as a protective adaptation against water loss under arid conditions (Kausar et al., 2012; Kaleem and Hameed, 2021; Terletskaya et al., 2022).

In saline desert (SD) populations, large vascular bundles coupled with increased xylem and phloem activity contribute to increased water, mineral and photosynthate contents (Iqbal et al., 2021). Consequently, these adaptations contribute to improved survival capabilities in hyper-saline habitats (Mumtaz et al., 2021; Sarwar et al., 2022). Stomatal density, which is closely linked to photosynthetic activity and energy production, also increased, while stomatal area decreased, particularly in the Coarse sand desert population (CS) (Table 3, Fig. 8). This adaptation is beneficial for stomatal regulation, controlling transpiration and maintaining cell turgidity under water deficit soil conditions (Ahmad et al., 2023).

4.5. Phytoremediation: viable ecological strategy of *Suaeda vera* in saline environments

This study highlights the ecological adaptive strategies of halophytes, which aligns with their phytoremediation potential across different salinity levels. A relatively high bioconcentration (BCF) serves as a key indicator of a plant's ability to accumulate salts within its aerial parts (Asghar et al., 2023; Naz et al., 2024; Abid et al., 2025), whereas an increased TF indicates the effective translocation of salts from the

roots to the above-ground parts. The BCF values for root Na^+ and Cl^- remained below 1 across all habitats, suggesting limited salt accumulation in the roots. In contrast, the shoot Na^+ and Cl^- BCF values exceeded 1 or approached 1 in all habitats except DD and RD, indicating the predominant salt accumulation in the shoots. The translocation factor (TF) for both Na^+ and Cl^- increased with salinity, and reached a maximum in high saline (SD, SW) populations, indicating efficient ion movement from the soil to the roots and subsequently to the leaves, facilitating their compartmentalization into vacuoles (Asghar et al., 2023). The high dilution factor of shoot Na^+ and Cl^- along with the lower root dilution factor, further confirmed salt compartmentalization within leaf vacuoles in highly saline (SD, SW) populations (Table 4). These traits can effectively be used to evaluate potential halophytic plant species for phytoremediation of salt affected lands and suggest that further research on genetic traits and functional responses related to salinity tolerance could contribute to the ecological success of this species in hypersaline environments (Iqbal et al., 2022; Bibi et al., 2024; Irshad et al., 2024).

5. Conclusion

This study revealed substantial phenotypic plasticity in *Suaeda vera* populations across diverse saline habitats, highlighting their ecological adaptability through specific morpho-anatomical and physiological traits. Key adaptations included elevated ion uptake, effective salt translocation and compartmentalization, enhanced growth attributes, increased organic osmolytes, elevated antioxidant enzyme activities, and specialized structural features. Highly saline populations (SD, SW, and SI) exhibited high bioconcentration and translocation of Na^+ and Cl^- in shoots along with increased succulence, highlighting the potential role of *Suaeda vera* in effectively remediating saline soils with a salinity level of up to 39.75 dS m^{-1} . While promising for soil reclamation, further statistically rigorous and long-term field validations are recommended to confirm practical applications.

CRediT authorship contribution statement

Naila Asghar: Writing – original draft, Methodology, Conceptualization. **Zhen Liu:** Project administration, Investigation, Formal analysis. **Amina Ameer:** Software, Formal analysis, Data curation. **Khawaja Shafique Ahmad:** Software, Data curation. **Ummar Iqbal:** Software. **Mansoor Hameed:** Supervision. **Ying Shen:** Software. **Zhao Hongxiang:** Formal analysis. **Muhammad Kaleem:** Software. **Tangyuan Ning:** Writing – review & editing, Resources, Project administration, Funding acquisition.

Declaration of competing interest

The authors declares no conflicts of interest.

Acknowledgements

This work was jointly supported by the Major Science and Technology Innovation Projects of Shandong Province (Grant No. 2022TZXD0038) and the National Key R&D Program of China (2023YFD2001400).

Data availability

Data will be made available on request.

References

- Abd El-Maboud, M.M., Khalil, R.M., 2013. Ecophysiological and genetic studies on some species of the genus *Suaeda* Forsk ex Scop. in the Mediterranean Sea coast. World Appl. Sci. J. 27, 811–825. <https://doi.org/10.5829/idosi.wasj.2013.27.07.13669>.

- Abid, H., Mahroof, S., Ahmad, K.S., Mehmood, A., Shehzad, M.A., Basit, A., Sadia, S., Iqbal, U., Tahir, M.M., Awan, U.A., Almutairi, K.F., Elansary, H.O., Moussa, I.M., 2025. Harnessing native plants for sustainable heavy metal phytoremediation in crushing industry soils of Muzaffarabad. *Environ. Technol. Innov.* 38, 104141. <https://doi.org/10.1016/j.eti.2025.104141>.
- Ahmad, R., Khuroo, A.A., Hamid, M., Malik, A.H., Rashid, I., 2019. Scale and season determine the magnitude of invasion impacts on plant communities. *Flora* 260, 151481. <https://doi.org/10.1016/j.flora.2019.151481>.
- Ahmad, I., Sohal, M., Hameed, M., Fatima, S., Ahmad, M.S.A., Ahmad, F., Ahmad, A., Mehmood, A., Basharat, S., Asghar, A., Shah, S.M.R.A., Ahmad, K.S., 2023. Morpho-anatomical determinants of yield potential in *Olea europaea* L. cultivars belonging to diversified origin grown in semi-arid environments. *PLoS One* 18, e0286736. <https://doi.org/10.1371/journal.pone.0286736>.
- Akhtar, N., Hameed, M., Nawaz, F., Ahmad, K.S., Hamid, A., Segovia-Salcedo, C., Shahnaz, M.M., 2017. Leaf anatomical and biochemical adaptations in *Typha domingensis* Pers. ecotypes for salinity tolerance. *Bot. Sci.* 95, 807–821. <https://doi.org/10.1111/bots.12886>.
- Alam, P., Albalawi, T.H., Altalayan, F.H., Bakht, M.A., Ahanger, M.A., Raja, V., Ahmad, P., 2019. 24-Epibrassinolide (EBR) confers tolerance against NaCl stress in soybean plants by up-regulating antioxidant system, ascorbate-glutathione cycle, and glyoxalase system. *Biomolecules* 9, 640. <https://doi.org/10.3390/biom9110640>.
- Ameer, A., Ahmad, F., Asghar, N., Hameed, M., Ahmad, K.S., Mehmood, A., Nawaz, F., Shehzad, A., Mumtaz, S., Kaleem, K., Iqbal, U., 2023. Aridity-driven changes in structural and physiological characteristics of Buffel grass (*Cenchrus ciliaris* L.) from different ecozones of Punjab, Pakistan. *Physiol. Mol. Biol. Plants* 29, 1205–1224. <https://doi.org/10.1007/s12298-023-01351-3>.
- Arnon, D.I., 1949. Copper enzymes in isolated chloroplasts: polyphenoloxidase in *Beta vulgaris*. *Plant Physiol.* 24, 1–15. <https://doi.org/10.1104/pp.24.1.1>.
- Asghar, N., Hameed, M., Ahmad, M.S.A., 2023. Ion homeostasis in differently adapted populations of *Suaeda vera* Forssk. ex J.F. Gmel. for phytoremediation of hypersaline soils. *Int. J. Phytoremediation* 25, 47–65. <https://doi.org/10.1080/15226514.2022.2056134>.
- Atzori, G., de Vos, A.C., van Rijsselbergh, M., Vignolini, P., Rozema, J., Mancuso, S., van Bodegom, P.M., 2017. Effects of increased seawater salinity irrigation on growth and quality of the edible halophyte *Mesembryanthemum crystallinum* L. under field conditions. *Agric. Water Manag.* 187, 37–46. <https://doi.org/10.1016/J.AGWAT.2017.03.020>.
- Basharat, S., Ahmad, F., Hameed, M., Ahmad, M.S.A., Asghar, A., Fatima, S., Abbas, Z., 2024. Structural and functional strategies in *Cenchrus* species to combat environmental extremities imposed by multiple abiotic stresses. *Plants* 13, 203. <https://doi.org/10.3390/plants13020203>.
- Bates, L.S., Waldren, R.P., Teare, I.D., 1973. Rapid determination of free proline for water-stress studies. *Plant Soil* 39, 205–207. <https://doi.org/10.1007/BF00018060>.
- Ben Hamed, K., Chibani, F., Abdelly, C., Magne, C., 2016a. Growth, sodium uptake and antioxidant responses of coastal plants differing in their ecological status under increasing salinity. *Biologia* 69, 193–201. <https://doi.org/10.2478/s11756-013-0304-1>.
- Ben Hamed, K., Hamad, I.B., Bouteau, F., Abdelly, C., 2016b. Insights into the ecology and the salt tolerance of the halophyte *Cakile maritima* using multidisciplinary approaches. In: *Halophytes for Food Security in Dry Lands*. Academic Press, pp. 197–211. <https://doi.org/10.1016/B978-0-12-801854-5.00012-4>.
- Bibi, S., Ahmad, M.S.A., Hameed, M., Alvi, A.K., 2024. Water conservation strategies in big cordgrass (*Desmostachya bipinnata* L.) for ecological success in hyper-arid and saline-arid environments. *Arid Land Res. Manag.* 38, 81–96. <https://doi.org/10.1080/15324982.2023.2270831>.
- Bistgani, Z.E., Hashemi, M., DaCosta, M., Craker, L., Maggi, F., Morshedloo, M.R., 2019. Effect of salinity stress on the physiological characteristics, phenolic compounds and antioxidant activity of *Thymus vulgaris* L. and *Thymus daenensis* Celak. *Ind. Crops Prod.* 135, 311–320. <https://doi.org/10.1016/j.indcrop.2019.04.055>.
- Boestfleisch, C., Papenbrock, J., 2017. Changes in secondary metabolites in the halophytic putative crop species *Crithmum maritimum* L., *Triglochin maritima* L. and *Halimione portulacoides* (L.) Aellen as reaction to mild salinity. *PLoS One* 12, e0176303. <https://doi.org/10.1371/journal.pone.0176303>.
- Certain, C., Della Patrona, L., Gunkel-Grillon, P., Léopold, A., Soudant, P., Le Grand, F., 2021. Effect of salinity and nitrogen form in irrigation water on growth, antioxidants and fatty acids profiles in halophytes *Salsola australis*, *Suaeda maritima*, and *Enchyliena tomentosa* for a perspective of biosaline agriculture. *Agronomy* 11, 449. <https://doi.org/10.3390/agronomy11030449>.
- Chakraborty, K., Basak, N., Bhaduri, D., Ray, S., Vijayan, J., Chattopadhyay, K., Sarkar, R.K., 2018. Ionic basis of salt tolerance in plants: nutrient homeostasis and oxidative stress tolerance. In: Hossain, M.A., Kumar, V., Burritt, D.J., Fujita, M., Mäkelä, P.S.A. (Eds.), *Plant Nutrients and Abiotic Stress Tolerance*. Springer, Cham, pp. 325–362. https://doi.org/10.1007/978-3-319-94096-3_13.
- Chance, B., Maehly, A.C., 1955. Assay of catalases and peroxidases. *Methods Enzymol.* 2, 764–775. [https://doi.org/10.1016/S0076-6879\(55\)02300-8](https://doi.org/10.1016/S0076-6879(55)02300-8).
- Davis, B.H., 1977. Carotenoids in higher plants. In: Chapman, D., Hall, L. (Eds.), *Lipids and Lipid Polymers in Higher Plants*. Springer, Berlin, Heidelberg, pp. 199–217. https://doi.org/10.1007/978-3-642-66632-2_11.
- Diwan, H., Ahmad, A., Iqbal, M., 2010. Uptake-related parameters as indices of phytoremediation potential. *Biologia* 65 (6), 1004–1011. <https://doi.org/10.2478/s11756-010-0106-7>.
- Eisa, S.S., Eid, M.A., Abd El-Samad, E.H., Hussin, S.A., Abdel-Ati, A.A., El-Bordeny, N.E., Ali, S.H., Alsayed, H.M.A., Lotfy, M.E., Masoud, A., El-Nagar, A.M., Ebrahim, M., 2017. *Chenopodium quinoa* Willd.: a new cash crop halophyte for saline regions of Egypt. *Aust. J. Crop. Sci.* 11, 343–351. <https://doi.org/10.21475/ajcs.17.11.03.316>.
- Fatima, S., Hameed, M., Naz, N., Shah, S.M.R., Naseer, M., Aqeel, S., Ashraf, M., Ahmad, F., Ahmad, I., 2021. Survival strategies in khavi grass [*Cymbopogon jwarancusa* (Jones) Schult.] colonizing hot hypersaline and arid environments. *Water, Air, Soil Pollut.* 232, 82. <https://doi.org/10.1007/s11270-021-05050-1>.
- Flowers, T.J., Colmer, T.D., 2008. Salinity tolerance in halophytes. *New Phytol.* 179, 945–963. <https://doi.org/10.1111/j.1469-8137.2008.02531.x>.
- Gautam, R.K., Singh, R.K., Krishnamurthy, S.L., Singla-Pareek, S.L., 2024. Enhancing salinity tolerance in crops—molecular and practical perspectives. *Front. Plant Sci.* 15, 1367677. <https://doi.org/10.3389/fpls.2024.1367677>.
- Giannopolitis, C.N., Ries, S.K., 1977. Superoxide dismutases: occurrence in higher plants. *Plant Physiol.* 59, 309–314. <https://doi.org/10.1104/pp.59.2.309>.
- Haque, M.I., Siddiqui, S.A., Jha, B., Rathore, M.S., 2021. Interactive effects of abiotic stress and elevated CO₂ on physio-chemical and photosynthetic responses in *Suaeda* species. *J. Plant Growth Regul.* 41, 2930–2948. <https://doi.org/10.1007/s00344-021-10485-1>.
- Hossain, M.S., 2019. Present scenario of global salt-affected soils, its management and importance of salinity research. *Int. Res. J. Biol. Sci.* 1, 1–3. <https://doi.org/10.2478/irjbs.2019.1.3>.
- Iqbal, U., Hameed, M., Ahmad, F., 2021. Water conservation strategies through anatomical traits in the endangered arid zone species *Salvadora oleoides* Decne. *Turk. J. Bot.* 45, 140–157. <https://doi.org/10.3909/bot.2010-42>.
- Iqbal, U., Hameed, M., Ahmad, F., Ahmad, M.S.A., Ashraf, M., 2022. Unraveling the survival potential of a desert halophyte *Salvadora oleoides* Decne. across heterogenous environments. *Trees (Berl.)* 36, 1085–1104. <https://doi.org/10.1007/s00468-022-02286-8>.
- Iqbal, U., Hameed, M., Ahmad, F., Ahmad, M.S.A., Naz, N., Ashraf, M., Kaleem, M., 2023a. Modulation of structural and functional traits in facultative halophyte *Salvadora oleoides* Decne. for adaptability under hyper-arid and saline environments. *J. Arid Environ.* 213, 104965. <https://doi.org/10.1016/j.jaridenv.2023.104965>.
- Iqbal, U., Hameed, M., Ahmad, F., Ahmad, M.S.A., Ashraf, M., 2023b. Fate of rubber bush (*Calotropis procera* (Aiton) W.T. Aiton) in adversary environment modulated by microstructural and functional attributes. *J. Arid Land* 15, 578–601. <https://doi.org/10.1007/s40333-023-0104-y>.
- Irshad, M., Hameed, M., Iqbal, U., Kaleem, M., Ameer, A., Asghar, N., Ahmad, K.S., 2024. Elevation-driven modifications in tissue architecture and physiobiochemical traits of *Panicum antidotale* Retz in the Pothohar Plateau, Pakistan. *Plant Stress* 11, 100430. <https://doi.org/10.1016/j.stress.2023.100430>.
- Isayenkov, S.V., Maathuis, F.J., 2019. Plant salinity stress: many unanswered questions remain. *Front. Plant Sci.* 10, 80. <https://doi.org/10.3389/fpls.2019.00080>.
- Jackson, M.L., 1962. *Soil Chemical Analysis*. Constable and Co. Ltd., London, pp. 1–498.
- Joshi, S., Nath, J., Singh, A.K., Pareek, A., Joshi, R., 2022. Ion transporters and their regulatory signal transduction mechanisms for salinity tolerance in plants. *Physiol. Plantarum* 174, e13702. <https://doi.org/10.1111/ppl.13702>.
- Joshi, A., Rajput, V.D., Verma, K.K., Minkina, T., Ghazaryan, K., Arora, J., 2023. Potential of *Suaeda nudiflora* and *Suaeda fruticosa* to adapt to high salinity conditions. *Horticulturae* 9, 1. <https://doi.org/10.3390/horticulturae9010074>.
- Kader, M.A., Lindberg, S., 2005. Uptake of sodium in protoplasts of salt-sensitive and salt-tolerant cultivars of rice, *Oryza sativa* L., determined by the fluorescent dye SBFI. *J. Exp. Bot.* 56, 3149–3158. <https://doi.org/10.1093/jxb/eri322>.
- Kaleem, M., Hameed, M., 2021. Structural and functional modifications in *Fimbristylis Vahl* for ecological fitness in hyper-saline wetlands. *Wetl. Ecol. Manag.* 29, 843–865. <https://doi.org/10.1007/s11273-021-09874-2>.
- Kaleem, M., Hameed, M., Ahmad, F., Ashraf, M., Ahmad, M.S.A., 2022. Anatomical and physiological features modulate ion homeostasis and osmoregulation in aquatic halophyte *Fimbristylis complanata* (Retz.) link. *Acta Physiol. Plant.* 44, 59. <https://doi.org/10.1007/s11738-022-03367-2>.
- Kausar, A., Ashraf, M.Y., Ali, I., Niaz, M., Abbass, Q., 2012. Evaluation of sorghum varieties/lines for salt tolerance using physiological indices as screening tool. *Pakistan J. Bot.* 44 (1), 47–52. <https://doi.org/10.30848/PJB2022-44>.
- Khan, M.A., Weber, D.J., 2006. Ecophysiology of High Salinity Tolerant Plants, vol. 40. Springer Science & Business Media. <https://doi.org/10.1007/978-1-4020-4957-0>.
- Khan, M.A., Ungar, I.A., Showalter, A.M., 2005. Salt stimulation and tolerance in an intertidal stem-succulent halophyte. *J. Plant Nutr.* 28, 1365–1374. <https://doi.org/10.1080/01904160500327384>.
- Khan, H.A., Siddique, K.H., Munir, R., Colmer, T.D., 2015. Salt sensitivity in chickpea: growth, photosynthesis, seed yield components and tissue ion regulation in contrasting genotypes. *J. Plant Physiol.* 182, 1–12. <https://doi.org/10.1016/j.jplph.2015.05.004>.
- Kowalenko, C.G., Lowe, L.E., 1973. Determination of nitrates in soil extracts. *Soil Sci. Soc. Am. J.* 37, 660. <https://doi.org/10.2136/sssaj1973.03615995003700040035x>.
- Liu, L., Nakamura, Y., Taliman, N.A., Sabagh, A.E., Moghaieb, R.E., Saneoka, H., 2020. Differences in the growth and physiological responses of the leaves of *Peucedanum japonicum* and *Hordeum vulgare* exposed to salinity. *Agriculture* 10, 317. <https://doi.org/10.3390/agriculture10090317>.
- Loconsole, D., Amador, B., Cristiano, G., Lucia, B., 2019. Halophyte common ice plants: a future solution to arable land salinization. *Sustainability* 11, 6076. <https://doi.org/10.3390/su11216076>.
- Maathuis, F.J., Ahmad, I., Patishian, J., 2014. Regulation of Na⁺ fluxes in plants. *Front. Plant Sci.* 5, 467. <https://doi.org/10.3389/fpls.2014.00467>.
- Mahmood, A., Latif, T., Khan, M.A., 2009. Effect of salinity on growth, yield, and yield components in basmati rice germplasm. *Pakistan J. Bot.* 41, 3035–3045. [https://doi.org/10.30848/PJB2009-41\(6\)8](https://doi.org/10.30848/PJB2009-41(6)8).
- Mahmuda, B.M., Datta, J., Rohman, M.M., Hasanuzzaman, M., Hossain, A., Islam, M.S., Bukhari, M.A., Jabeen, T., Mubeen, M., Nasim, W., Rehman, A., Ratnasekera, D.,

- Llanes, A., Athar, H., Iqbal, M.A., Ahmed, S., Gill, R.A., Hadifa, A., Ueda, A., Liu, L., Skalicky, M., Brešić, M., Erman, M., Kaya, Y., Sabagh, A.E., 2022. Saline toxicity and antioxidant response in *Oryza sativa*: an updated review. In: Managing Plant Production Under Changing Environment. Springer, pp. 79–102. https://doi.org/10.1007/978-981-16-5059-8_4.
- Maimaitiyiming, M., Ghulam, G.A., Bozzolo, A., Wilkins, J.L., Kwasniewski, M.T., 2017. Early detection of plant physiological responses to different levels of water stress using reflectance spectroscopy. *Remote Sens.* 9, 745. <https://doi.org/10.3390/rs9070745>.
- Mansoor, U., Fatima, S., Hameed, M., Naseer, M.S.A., Ahmad, M., Ashraf, M., Ahmad, F., Waseem, M., 2019. Structural modifications for drought tolerance in stem and leaves of *Cenchrus ciliaris* L. ecotypes from the Cholistan Desert. *Flora* 261, 151485. <https://doi.org/10.1016/j.flora.2019.151485>.
- Moore, S., Stein, W.H., 1948. Photometric ninhydrin method for use in the chromatography of amino acids. *J. Biol. Chem.* 176, 367–388.
- Muchate, N.S., Nikalje, G.C., Rajurkar, N.S., Suprasanna, P., Nikam, T.D., 2016. Physiological responses of the halophyte *Sesuvium portulacastrum* to salt stress and their relevance for saline soil bio-reclamation. *Flora* 224, 96–105. <https://doi.org/10.1016/j.flora.2016.02.009>.
- Mujeeb, A., Abideen, Z., Aziz, I., Sharif, N., Hussain, M.I., Qureshi, A.S., Yang, H.H., 2023. Phytoremediation of potentially toxic elements from contaminated saline soils using *Salvadora persica* L.: seasonal evaluation. *Plants* 12, 598. <https://doi.org/10.3390/plants12030598>.
- Mumtaz, S., Saleem, M.H., Hameed, M., Batool, F., Parveen, A., Amjad, S.F., Mahmood, A., Arfan, M., Ahmed, S., Yasmin, H., Alsahl, A.A., Alyemeni, M.N., 2021. Anatomical adaptations and ionic homeostasis in aquatic halophyte *Cyperus laevigatus* L. under high salinities. *Saudi J. Biol. Sci.* 28, 2655–2666. <https://doi.org/10.1016/j.sjbs.2020.12.024>.
- Naskar, S., Palit, P.K., 2015. Anatomical and physiological adaptations of mangroves. *Wetl. Ecol. Manag.* 23, 357–370. <https://doi.org/10.1007/s11273-015-9391-5>.
- Naz, N., Fatima, S., Hameed, M., Ashraf, M., Ahmad, M.S.A., Ahmad, F., Shah, S.M.R., Islam, F., Ahmad, I., Ejaz, F., Naseer, M., 2022. Contribution of structural and functional adaptations of hyper-accumulator *Suaeda vera* Forssk. ex J.F. Gmel. for adaptability across salinity gradients in hot desert. *Environ. Sci. Pollut. Res.* 29, 64077–64095. <https://doi.org/10.1007/s11356-022-19167-1>.
- Naz, N., Asghar, A., Basharat, S., Fatima, S., Hameed, M., Ahmad, M.S.A., Ashraf, M., 2024. Phytoremediation through microstructural and functional alterations in alkali weed (*Cressa cretica* L.) in the hyperarid saline desert. *Int. J. Phytoremediation* 26, 913–927. <https://doi.org/10.1080/15226514.2023.2246571>.
- Ogburn, R.M., Edwards, E.J., 2010. The ecological water-use strategies of succulent plants. *Adv. Bot. Res.* 55, 179–225. [https://doi.org/10.1016/S0065-2296\(10\)55005-2](https://doi.org/10.1016/S0065-2296(10)55005-2).
- Pan, Y.Q., Guo, H., Wang, S.M., Zhao, B., Zhang, J.L., Ma, Q., Bao, A.K., 2016. The photosynthesis, Na⁺/K⁺ homeostasis and osmotic adjustment of *Atriplex canescens* in response to salinity. *Front. Plant Sci.* 7, 848. <https://doi.org/10.3389/fpls.2016.00848>.
- Parida, A.K., Veerabathini, S.K., Kumari, A., Agarwal, P.K., 2016. Physiological, anatomical and metabolic implications of salt tolerance in the halophyte *Salvadora persica* under hydroponic culture condition. *Front. Plant Sci.* 7, 351. <https://doi.org/10.3389/fpls.2016.00351>.
- Rahneshan, Z., Nasibi, F., Moghadam, A.A., 2018. Effects of salinity stress on some growth, physiological, biochemical parameters and nutrients in two pistachio (*Pistacia vera* L.) rootstocks. *J. Plant Interact.* 13, 73–82. <https://doi.org/10.1080/17429145.2018.1439790>.
- Roy, S.J., Negrao, S., Tester, M., 2014. Salt resistant crop plants. *Curr. Opin. Biotechnol.* 26, 115–124. <https://doi.org/10.1016/j.copbio.2013.12.002>.
- Rozema, J., Schat, H., 2013. Salt tolerance of halophytes, research questions reviewed in the perspective of saline agriculture. *Environ. Exp. Bot.* 92, 83–95. <https://doi.org/10.1016/j.envexpbot.2012.11.004>.
- Safdar, H., Amin, A., Shafiq, Y., Ali, A., Yasin, R., Shoukat, A., Hussan, M.U., Sarwar, M. I., 2019. A review: impact of salinity on plant growth. *Nat. Sci.* 17 (1), 34–40. <https://doi.org/10.4236/ns.2019.171005>.
- Sarwar, Y., Asghar, A., Hameed, M., Fatima, S., Ahmad, F., Ahmad, M.S.A., Ashraf, M., Shah, S.M.R., Basharat, S., Iqbal, U., Irshad, M., Ahmad, I., 2022. Structural responses of differentially adapted *Cenchrus setigerus* Vahl ecotypes to water deficit. *Environ. Exp. Bot.* 194, 104746. <https://doi.org/10.1016/j.envexpbot.2022.104746>.
- Shaar-Moshe, L., Blumwald, E., Peleg, Z., 2017. Unique physiological and transcriptional shifts under combinations of salinity, drought, and heat. *Plant Physiol.* 174, 421–434. <https://doi.org/10.1104/pp.16.01676>.
- Shi, L., Zhu, X., Qian, T., Du, J., Du, Y., Ye, J., 2023. Mechanism of salt tolerance and plant growth promotion in *Priestia megaterium* ZS-3 revealed by cellular metabolism and whole-genome studies. *Int. J. Mol. Sci.* 24, 15751. <https://doi.org/10.3390/ijms24235751>.
- Song, J., Wang, B., 2015. Using euhalophytes to understand salt tolerance and to develop saline agriculture: *Suaeda salsa* as a promising model. *Ann. Bot.* 115 (3), 541–553. <https://doi.org/10.1093/aob/mcu232>.
- Surówka, E., Hura, T., 2020. Osmoprotectants and nonenzymatic antioxidants in halophytes. In: Handbook of Halophytes: from Mol. to Ecosyst. Towards Biosaline Agric. (2020), pp. 1–31. https://doi.org/10.1007/978-3-030-57635-6_78.
- Tang, X., Mu, X., Shao, H., Wang, H., Brešić, M., 2015. Global plant-responding mechanisms to salt stress: physiological and molecular levels and implications in biotechnology. *Crit. Rev. Biotechnol.* 35, 425–437. <https://doi.org/10.3109/07388551.2014.938754>.
- Tavakkoli, E., Rengasamy, P., McDonald, G.K., 2010. High concentrations of Na⁺ and Cl⁻ ions in soil solution have simultaneous detrimental effects on growth of faba bean under salinity stress. *J. Exp. Bot.* 61, 4449–4459. <https://doi.org/10.1093/jxb/erq240>.
- Terleetskaya, N.V., Erbay, M., Zorbekova, A.N., Prokofieva, M.Y., Saidova, L.T., Mamirova, A., 2022. Influence of osmotic, salt, and combined stress on morphophysiological parameters of *Chenopodium quinoa* photosynthetic organs. *Agriculture* 13, 1. <https://doi.org/10.3390/agriculture13010001>.
- Thorup-Kristensen, K., Halberg, N., Nicolaisen, M., Olesen, J.E., Crews, T.E., Hinsinger, P., Dresbøll, D.B., 2020. Digging deeper for agricultural resources, the value of deep rooting. *Trends Plant Sci.* 25, 406–417. <https://doi.org/10.1016/j.tplants.2019.12.007>.
- Wolf, B., 1982. An improved universal extracting solution and its use for diagnosing soil fertility. *Commun. Soil Sci. Plant Anal.* 13, 1005–1033. <https://doi.org/10.1080/00103628209367305>.
- Yemm, E.W., Willis, A.J., 1954. Stomatal movements and changes of carbohydrate in leaves of *Chrysanthemum maximum*. *New Phytol.* 53, 373–396. <https://doi.org/10.1111/j.1469-8137.1954.tb05242.x>.
- Yoshida, S., Forno, D.A., Cock, J.H., 1976. *Lab. Manual Phys. Stud. Rice*.
- You, J., Chan, Z., 2015. ROS regulation during abiotic stress responses in crop plants. *Front. Plant Sci.* 6, 1092. <https://doi.org/10.3389/fpls.2015.01092>.
- Yuan, F., Xu, Y., Leng, B., Wang, B., 2019. Beneficial effects of salt on halophyte growth: morphology, cells, and genes. *Open Life Sci.* 14, 191–200. <https://doi.org/10.1515/biol-2019-0021>.
- Zörb, C., Geilfus, C.M., Dietz, K.J., 2019. Salinity and crop yield. *Plant Biol.* 21, 31–38. <https://doi.org/10.1111/plb.12903>.
- Zulfiqar, F., Younis, A., Riaz, A., Mansoor, F., Hameed, M., Akram, N.A., Abideen, Z., 2020. Morpho-anatomical adaptations of two *Tagetes erecta* L. cultivars with contrasting response to drought stress. *Pakistan J. Bot.* 52, 801–810. [https://doi.org/10.30848/PJB2020-3\(35](https://doi.org/10.30848/PJB2020-3(35)